A probabilistic model to evaluate the effectiveness of main solutions to COVID-19 spreading in university buildings according to proximity and time-based consolidated criteria

Marco D'Orazio
DICEA-Università Politecnica delle Marche https://orcid.org/0000-0003-3779-4361
Gabriele Bernardini
DICEA-Università Politecnica delle Marche https://orcid.org/0000-0002-7381-4537
Enrico Quagliarini (e.quagliarini@staff.univpm.it)
DICEA-Università Politecnica delle Marche https://orcid.org/0000-0002-1091-8929

Research Article

Keywords: simulation model, closed built environment, building occupancy, crowd models, proximity exposure, COVID-19

Posted Date: September 25th, 2020

DOI: https://doi.org/10.21203/rs.3.rs-82941/v1

A probabilistic model to evaluate the effectiveness of main solutions to COVID-19 spreading in university buildings according to proximity and time-based consolidated criteria

Marco D'Orazio[1], Gabriele Bernardini[1], Enrico Quagliarini[1]

[1] DICEA Dept, Università Politecnica delle Marche, via di Brecce Bianche 60131 Ancona, phone: +39 071 220 4246, fax: +39 071 220 4582, mail: e.quagliarini@staff.univpm.it

Abstract. Crowds in buildings open to the public can alter the occupants' safety in different emergency conditions, including those related to a pandemic. In this sense, university buildings are one of the most relevant scenarios in which the COVID-19 event clearly pointed out the stakeholders' needs toward safety issues, especially because of the possibility of day-to-day presences of the same users (i.e. students, teachers) and overcrowding causing long-lasting contacts with possible "infectors" in such closed environments. While waiting for the vaccine, as for other public buildings, policy-makers' measures to limit (second) virus outbreaks combine individual's strategies (facial masks), occupants' capacity and access control to avoid lockdowns and ensure adequate conditions for occupants. Simulators could support effectiveness evaluations of such measures. To fill this gap, this work proposes a quick and probabilistic simulation model based on consolidated proximity and exposure-time-based rules for virus transmission (confirmed by international health organizations). The building occupancy is defined according to university schedule, identifying the main "attraction areas" in the building (classrooms, break-areas). Scenarios are defined in terms of occupants' densities, mitigation strategies, virus-related aspects. The model is calibrated on experimental data and applied to a relevant university building. Results demonstrate the model capabilities. In the case study, occupants' capacity limitation could support the adoption of surgical masks by users instead of FFPk masks (thus improving users' comfort issues). Preliminary correlations to combine acceptable mask filters-occupants' density are proposed to support stakeholders in organizing users' presences in the building during the pandemic.

Keywords. simulation model; closed built environment; building occupancy; crowd models; proximity exposure; COVID-19

1. Introduction

Buildings open to the public are critical scenarios for the safety of the occupants, especially when crowd conditions occur (Dong et al. 2018), and including those related to emergency events like a pandemic (Ronchi and Lovreglio 2020). The COVID-19 pandemic evidences how some issues in buildings fruition due to the long-lasting presence of people in closed built environment increase the pandemic spreading (Cirrincione et al. 2020; Zizzo et al. 2020; Wang et al. 2020; Ronchi and Lovreglio 2020). As a consequence, policy makers and stakeholders were leaded to control the access to the buildings (mainly, by limiting the building occupancy) and even promote compulsory and widespread lockdowns, thus causing disruption of activities (Anderson et al. 2020; Bruinen de Bruin et al. 2020). University buildings were (and still are) one of the most significant scenarios in this sense, causing disruption of Learning and Teaching (L&T) activities (Dohaney et al. 2020).

As for other public buildings, lockdowns of university buildings were provided to limit the exposure of the occupants to critical conditions (Anderson et al. 2020; Prem et al. 2020; Yang et al. 2020; Bruinen de Bruin et al. 2020) such as the long-lasting presence (day-to-day) of the same users (i.e. students, teachers): 1)in the same "attraction areas", where main L&T activities are carried out (classrooms), or occupants can have a break from their activities (break areas); 2) in possible overcrowding over time (e.g. due to the contemporary presence of the users in the main areas), which can seriously increase the probability of a user to be infected. Among the different exposure models in closed built environments (Ronchi and Lovreglio 2020), proximity-based and exposure time-based factors of virus transmission seem to be the most relevant and confirmed roles in respect to high-risk exposure/close contact definition, according to consolidate criteria of national and international health

organizations[1] (Anderson et al. 2020; Prem et al. 2020; Yang et al. 2020; Bruinen de Bruin et al. 2020). In fact, such literature bases define how a probable case is a person remaining "in a closed environment (e.g. classroom, meeting room, hospital waiting room, etc.) with a COVID-19 case for 15 minutes or more and at a distance of less than 2 m", whose conditions include any direct and indirect contact according to a proximity-based standpoint (Cirrincione et al. 2020; Zizzo et al. 2020). In this term, space occupancy issues represent leading elements for the evaluation of the contagion spreading, as also demonstrated by real-world cases of closed environments, where such possible effects on the occupants are underlined (see, e.g., the Diamond Princess cruise emergency) (Mizumoto and Chowell 2020; Fang et al. 2020). Nevertheless, lockdowns-based measures have been overcome because of their not sustainable impact for the community, and in particular for academic continuity in the view, e.g. of barriers and negative experiences of remote access to L&T (Dohaney et al. 2020; Favale et al. 2020) (Dohaney et al. 2020). Towards this goal, policy-makers moved towards the combination of three main categories of more feasible mitigation strategies for public buildings to maintain an acceptable level of COVID19 cases over time, avoiding secondary virus outbreaks (Howard et al. 2020; Fang et al. 2020; Prem et al. 2020; Wilder-Smith et al. 2020; Yang et al. 2020; Servick 2020; Murray et al. 2020; Cirrincione et al. 2020; Chen et al. 2020)[1]:

1. social distancing solutions, essentially aimed at limiting the occupants' number in the building, to increase the possibility of maintaining safety distances (i.e. ranging from 1m to 2m depending on National Guidelines);
2. the use of respiratory protective devices (facial masks), since a higher probability to be infected can be associated with the absence of individual's protection-based measures;
3. the control of COVID-19 infectors, starting from the detection of the symptoms (e.g. fever) to isolate the possible infected cases, up to the tracing of infected cases motion to limit

[1] e.g.: http://www.salute.gov.it/portale/nuovocoronavirus/dettaglioFaqNuovoCoronavirus.jsp?lingua=italiano&id=228 , https://www.ecdc.europa.eu/en/covid-19/surveillance/surveillance-definitions(last access: 5/8/2020);

their contact with susceptible people. In fact, the transmittal potential seems to increase in case of infectors' symptoms onset, as for other viruses.

Nevertheless, as for the other public buildings (Ronchi and Lovreglio 2020), decision makers in university building should understand the effective impact of each measure (and of their combination) to effectively set up acceptable solutions from the perspective of both the stakeholders (e.g. which solutions can be easily implemented with an effective impact on the activity?) and the final users (e.g. which solutions will lead to the possibility of restoring the "normal" fruition of the spaces?).

To this aim, simulation tools could be useful in predicting how different mitigation solutions could affect the virus spreading, as also remarked by previous studies on airborne diseases mitigation (Saari et al. 2006; Gao et al. 2008, 2016; Laskowski et al. 2011; Zhang et al. 2018). The importance of such tools has been evidenced in many different cases concerning individuals' safety in the built environment, including crowd conditions, such as those related to emergency safety and evacuation (Zheng et al. 2009; Casareale et al. 2017; Ronchi and Lovreglio 2020).

Concerning the COVID-19 emergency, different tools have been developed according to experimental data to derive general rules for the contagion spreading at a wide-scale (e.g. national scale) and the impact of risk-mitigation strategies on the number of infected people (Lopez and Rodo 2020; Prem et al. 2020; Fanelli and Piazza 2020), while limited efforts have been performed towards the definition of models in a closed environment (Mizumoto and Chowell 2020; Fang et al. 2020; Ronchi and Lovreglio 2020). As suggested by previous works (including simulation-based ones and those related to a wider scale context, e.g. city-scale) (Gao et al. 2016; Zhang et al. 2018; Prem et al. 2020), aspects related to the building occupancy (i.e. timing, probability to have close contacts in indoor spaces) will lead to one of the most significant contributions in the contagion spreading for the hosted users, because of the combination between occupancy timing, crowd level and social contacts ways (e.g. possibility of having close contacts/contacts within a radius of 2m for more than 15 minutes).

In view of the above, this study provides a simulation model to estimate the effectiveness of virus mitigation-measures to be adopted in university buildings. The modelling methodology adopts a probabilistic approach to the virus transmission based on statistics (in view of Susceptible-Infected models) (Banos et al. 2015) to merge virus spreading and individuals' (students and teachers') occupancy of the building spaces, under the following assumptions:

- *factors related to proximity and exposure-time for virus spreading are considered as priority elements for high-risk exposure/close contacts* as stated above[1], thus focusing on the most probable infections assessment. This approach allows representing the main drivers based on the distance between a virus carrier and the other individuals placed into the closed environment, including all direct and indirect spreading effects between two individuals all the main, as proposed by previous simulation models on COVID-19 (Fang et al. 2020; Yang et al. 2020; Ronchi and Lovreglio 2020). Other virus transmission modes connected to the presence of the individuals in the same room/building at the same time can exist (e.g. aerosol transmission route also due to ventilation effects) (Azimi et al. 2020; Dai and Zhao 2020), but: 1) to the date this paper was written (July 2020), they were not included in the main rules for international health organizations; 2) parameters to clearly evaluate their impact are still under development and validation (e.g. in view of applying Wells–Riley equation); 3) buildings in which the control of Indoor Air Quality is effective e.g. thanking to good ventilation systems, the infection probability due to aerosols seems to the limited to less than the 2%, thus provoking a very limited increase to the estimations due to close contacts (Dai and Zhao 2020). Behavioral issues which can impact on other contact-based transmission modes (i.e. indirect, by contaminated hands) are not here simulated also by considering general trends of population in awareness against such kind of virus transmission (Shiina et al. 2020);
- *the focus is given to "attraction areas" within the building*, since they are characterized by the most critical interactions between the occupants, usually for more than 15 minutes[1]. As previously stated, they are classrooms (where L&T is performed) and break areas, where people can stay

during the lesson breaks. Such quick-to-apply choice (which is shared with statistics-based SI models) does not aim at representing the individuals' desires in the space fruition which generally last less than 15 minutes (e.g. motion along building paths, specific interactions among users) from a microscopic standpoint (Ronchi and Lovreglio 2020), but the overall effects on the whole population, thanking to a wide sample of simulations which enhance the related statistic input data;

- in view of the above (i.e. not considering ventilation effects and individuals' motion), a specific representation of the space layout (e.g. introducing walls or other obstacles) is not here provided, since people can move between different *"attraction areas"* depending on the scheduling. The probabilistic approach enables to create different input scenarios in this sense and evaluate possible differences in the spreading trends from a statistical point of view.

The model is implemented through an agent-based simulation (Laskowski et al. 2011; D'Orazio et al. 2014; Banos et al. 2015) that allows characterizing the involved agent's rules in terms of "attraction areas" occupancy during the time and spreading-affecting additional features (i.e. occupants wearing a facial mask, being at a particular moment of the incubation period, being asymptomatic or not) (Mizumoto and Chowell 2020; Fang et al. 2020). The model is then calibrated according to a real-world case study (the "Diamond Princess cruise") so as to characterize the input parameters to fit the contagion spreading data and reduce the gaps due to additional effects of secondary (aerosol-based) transmission ways (Azimi et al. 2020; Mizumoto and Chowell 2020). Finally, the application of the calibrated model is provided for a significant university case study to evaluate the model capabilities in respect to different mitigation strategies by also providing insights on reliable solution combinations for building decision makers.

2. Phases, model description and methods

The work is divided into the following phases:

1) definition of the modelling approach (see Section 2.1);

2) implementation of the model within a simulation software, and calibration activities according to experimental data related to a significant closed environment (Diamond Princess case study) (see Section 2.2);
3) application to a relevant case study, by considering a sensitivity analysis-based approach, and then evaluating the impact of different spreading-mitigation strategies (i.e.: respiratory protective devices; crowd level control; infectors' access control) (see Section 2.3).

2.1. Modelling approach

The spreading of COVID-19 between the occupants into the closed environment of university buildings is modelled by jointly representing the occupancy of the building spaces considered as "attraction areas" for the users during L&T activities (i.e. classrooms, break areas) and the epidemic-related issues (Banos et al. 2015; Fang et al. 2020). To this end, a probabilistic (statistics-based) approach to virus transmission and occupancy tasks is adopted, by means of ABM techniques and tools to assign effective rules to the agent, over space and time (D'Orazio et al. 2014; Banos et al. 2015). A general schematization of the overall epidemiological model approach is resumed in Figure 1, while Table 1 resumes the model parameters discussed below.

Concerning the epidemic-related aspects, each simulated agent is characterized by:

- being infected or not, which can vary at each step of the simulation. When the simulation starts, there is a certain percentage of occupants that is infected inside the Built Environment. A latent period for infected agents can exist (Lauer et al. 2020), called "*delay*" period. Hence, once an individual is infected, he/she can become an *effective infector* after the initial *delay* period, which corresponds to the initial phase during which the virus load increases up to provoke secondary infections. The contagion timing is t^* [simulation step]. At $t^*=0$, the agent becomes infected. Then, $I_{delay}(t^*)$ [simulation step], which is defined as the current step from the virus contagion, increases at each simulation step by a *formcoeff* ($I_{delay}(t^*)=I_{delay}(t^*-1)+formcoeff$; in case of linear relationship, *formcoeff*=1). Hence, *formcoeff* expresses the speed of the process after the moment of the contagion;

- wearing or not a respiratory protective device (in the following: *mask*). The percentage of people wearing the *mask*, as well as the *mask* filtering capacity (defined according to European standard EN 149:2001), could be decided in the setup of the model.
- being asymptomatic or not after being infected. In particular, not asymptomatic people are considered to "die" (leave/not enter the building) when the current step from the virus contagion *Istep* [simulation step] reaches the timing to symptoms (e.g. fever) onset *Ifev* [simulation step] (Lauer et al. 2020). The agent's "die" behaviour could both represent the effects of the disease for: 1) people who can be blocked by building access control system; 2) people who spontaneously leave/not enter the building due to their health conditions.

At each simulation step, the model evaluates if an *effective infector* is placed near uninfected ones, assuming a radius of 2m as base proximity distance for contagion spreading *Dvir* [m], according to current consolidated rules provided by international health organizations[1]. In these conditions, each of the *effective infector i* has a chance to infect a neighbouring uninfected agent *j* according to Equation 1, which is based on previous modelling approaches (Fang et al. 2020):

$$Pvir = \min\left(1, i_j \cdot t_{exp} \cdot (1 - prot_i) \cdot (1 - prot_j) \cdot p_{imm}\right) \quad (1)$$

where:

- i_j is transmission efficiency [-] of the virus in the surrounding individual j, as in Equation 2. Simple linearity between the incubation-related inputs is assumed.

$$i = \min\left(1, \frac{Istep}{Iinc}\right) \quad (2)$$

- t_{exp} [-] is the normalized exposure time of *i* in respect of *j* as in Equation 3. It depends on the exposure time Δt [simulation step] and on the minimum contact time t_c [simulation step], which can provoke the virus spreading. t_c can be defined as the number of steps to simulate an equivalent time of 15 minutes. Simple linearity between the time-dependent inputs is assumed.

$$t_{exp} = min\left(1, \frac{\Delta t}{tc}\right) \quad (3)$$

- $prot_i$ and $prot_j$ [-] are the level of protection given by the *mask filter* of the facial *masks* worn by the two agents [-]. The parameters vary from 0, which implies "no mask", to 1, which corresponds to maximum protection level. More data on the *mask filter* values adopted by this study is provided in Table 1.
- p_{imm} [-] considers that "some people may be immune to the virus" (Fang et al. 2020), and it can vary from 0 to 1 (e.g., 0 corresponds to the case in which the whole population is vaccinated).

In Equation 1, the adoption of the term 1 as a comparison factor allows limiting the upper probability *Pvir* to 100%. Once *Pvir* has been calculated, a random number (varying from 0 to 1) is compared to *Pvir* to stochastically define *j* as a new infected agent when the random number is lower or equal than *Pvir*. Once the agent has become infected, he/she will change its status into *effective infector* when the *delay* value will be reached.

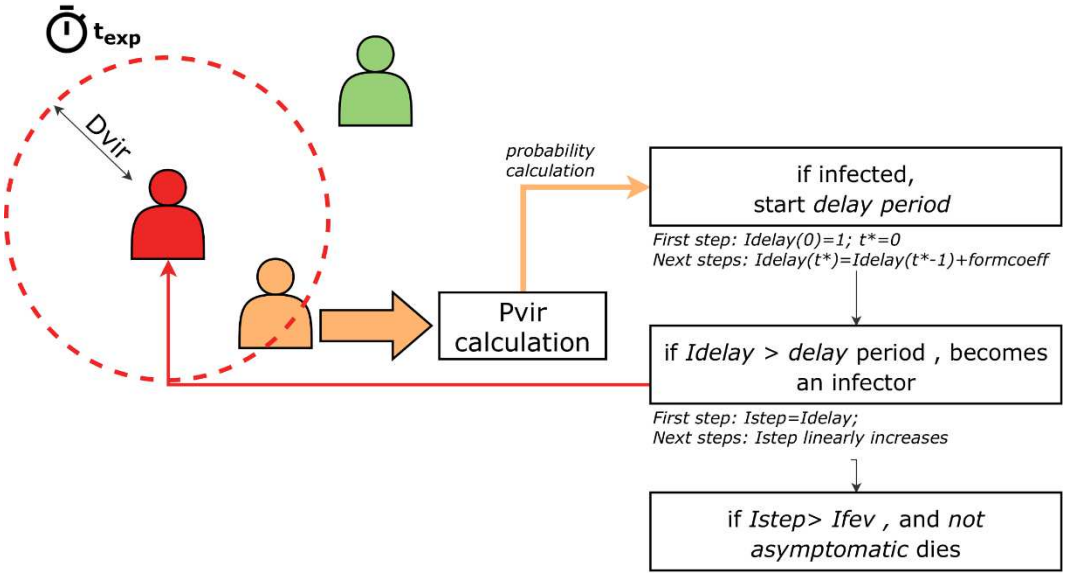

Figure 1. General scheme for the contagion spreading: the red agent is an infector, the green agent is out of Dvir, the orange agent is a possible infected agent. The Pvir calculation also depends on the exposure timing t_{exp}.

In view of the representation of occupancy-related tasks in the university building, the model considers that the agents are placed into a "close" *world*: there are no births and travel into or out of the simulated population, while deaths can exist because of the virus effects on the individuals. The

model is limited to the fact that: new infected can essentially occur inside the *world*; infected people can remain inside until to "die". Hence, the model could consider that the same daily users frequent the university building (Gao et al. 2016; Zhang et al. 2018): they can return home during the evening, but the following day they will share the building spaces with the other same users. *N* [pp] is the number of simulated agents into the *world*, and depends on the specific scenarios to be simulated. The *world* is characterized by "attraction areas" where the simulated agents can spend time according to the L&T activities schedule (classrooms and break areas), in view of an occupancy-based approach to building use and disease transmission .The classrooms are considered as the initial position where agents are generated, by considering an initial distance among the individuals randomly ranging from 1m to 3m, so as to respect the initial social distancing, that cannot be guaranteed all time long. Agents will spend most of the time in classrooms, having the possibility of leaving their initial position at the lessons breaks. In these moments, the individuals could reach a break area placed in a certain radius of space from the initial position (defined at the simulation setup). Then, after the break, they will return into the classroom, at their initial position. In this occupancy process, the agent could also not maintain the initial distance conditions, especially in case of significant occupants' loads in the considered building areas. The evaluation of classroom and break areas occupancy by the users is performed at given time steps, to simulate the possibility that the individuals spend a certain time near the same position during the lessons and at the lesson breaks. According to exposure time-based rules for the virus transmission, steps of 15 minutes are considered in this work, being consistent with typical university buildings scheduling (e.g. breaks duration between two lessons).

The probabilistic approach to the occupancy of an "attraction area" ensures that each simulated agent can randomly interact with his/her neighbors (by chance) according to the proximity-based rules for the contagion spreading. This occupancy-based approach to *Pvir* estimation is mainly affected by the density of the occupants placed in a certain area of the *world*, rather than on motion-related issues. Hence, the *world* area *A* [m^2] is estimated as the sum of "attraction areas", by using a patches-based representation: each patch is equal to 1m to consider a 1:1 scaled representation of the

building. Hence, the overall world area is codified according to a simplified squared area, with each side equal to $A^{1/2}$. By this way, it is possible to quickly recreate a unique layer for the whole *world*, to focus on the relationships between the individuals during the space occupancy.

Finally, the implemented model can allow agents to freely occupy or not the *world* space. In this second case (adopted for the case study), after the lesson break, the agent returns at the previous starting position in the *world* (e.g. within the initial classroom, and so within the same group of students). This essentially allows considering the agents' use of building spaces depending on the effective building schedule.

Parameter	**Unit of measure**	**Values range**	**Description**
N	pp	>0	number of people in the *world*
A	m^2, patches	>0	the dimension of the *world* in which the agents move
formcoeff	-	>0	speed of the virus spreading, by modifying the delay increase for each step
p_{imm}	%	0 to 100	If equal to 100%, all the population is virus-resistant (e.g. due to vaccine)
Initial infectors %	%	0 to 100	how many individuals could be infectors at the starting of the simulation
asymptomatic ratio	%	0 to 100	how many individuals could be infectors without symptoms, thus not "dying"
average delay	simulation steps	>0	the average delay between being an infected individual and an effective infector, due to virus replication dynamics (Lauer et al. 2020). It also depends on how many steps represent each simulation day.
Iinc	simulation step	>0	this is the incubation time, which starts from the contagion moment to the maximum considered display symptoms time (e.g. fever onset) for all the considered population (Lauer et al. 2020).
Ifev	simulation step	≥0	this is the time from the contagion to the minimum onset of the fever (compare to *Iinc*) (Lauer et al. 2020). In this work, the value is stochastically assigned within 0 to *Iinc*.
$prot_i$, $prot_j$ (*mask filter*)	-	0 to 1	specific values can be assigned for respiratory protective devices categories for filtering half masks given by EN 149:2009 by considering maximum aerosol drops penetration percentage. Single mask characterization ranges are considered to include superior limits for each kind of mask: FFP3≥98%, 98%>FFP2≥95%; 95%>FFP1≥80%.

			Besides, previous works tried to classify surgical mask efficiency according to the NIOSH NaCl method (Rengasamy et al. 2017), by providing an efficiency range from 54% to 88%. Finally, a no-protection limit for *mask filter* from 0 to 25% is selected to consider the non-standards protection solutions, basing on the first quartile in uniform input distribution.
t_c	simulation step	1 step = 15 minutes	number of steps to simulate an equivalent time of 15 minutes, according to consolidated data about indoor contagion spreading from national and international health organization[1]
mask wearing %	%	0 to 100	Percentage of people implementing the considered protection level $prot_i$
traveled distance	patches	≥1	maximum distance between the previous and the next occupancy task for each agent, that is considered between two different simulation steps. It can depend on the distance between the areas in which the individual spends time. The maximum distance could be ideally set at $A^{1/2}$ by considering a squared A in the patches description.

Table 1. Model parameters characterization

2.2. Model implementation and calibration

The model described in Section 2.1 is implemented in simulation software through NetLogo (Wilensky 1999). To ensure the application of statistical methods and the related reproducibility of scenarios in the calibration and application phases, an R script (R version 3.6.3[2]) is implemented to launch a series of simulation within the model according to previous research approaches on epidemiologic researches (Banos et al. 2015). Simulation runs were performed using NLRX package of "R statistics" programming language (Salecker et al. 2019), by defining the specific "experiment" conditions according to a series of input data

A preliminary simulation phase verified that no influence on the final result is provided by the initial distance among the simulated agents, as defined in Section 2.1. Then, the simulation model is then calibrated by comparing the simulation outputs and the experimental data of the contagion by the Diamond Princess cruise case study (Mizumoto and Chowell 2020). This environment represents

[2] https://cran.r-project.org/bin/windows/base/; last access: 17/4/2020

a "close" *world* and, essentially, a closed environment, according to the purposes of the proposed model.

The Diamond Princess cruise[3] is organized in 12 decks open to the passengers, with an overall length of about 290m, and calculated A of about 73500m^2. During the COVID-19 emergency onboard, the cruise host 3711 individuals. The index case was embarked on 20th of January 2020. On the 30th of January, a total of 2 observed cases were reported within the median incubation period (Lauer et al. 2020), and the index case was confirmed on 1st of February 2020. In this study, we consider the increase in observed cases from this day to the maximum daily values in "new" infected people (7th of February), according to the observed data from previous work on the cruise event (Mizumoto and Chowell 2020). Hence, the overall simulated time is equal to 7 days (420 steps according to Table 2 characterization). This comparison allows calibrating the speed of the virus spreading (analysis of the slope of the increasing part of the contagion curve) in the "close" simulated *world*. The *formcoeff* parameter is used to set up the general model in respect to the calibration reference without changing the general approach described in Section 2.1. Hence, if *formcoeff*=2, the process will ideally be twice faster than for *formcoeff*=1 (default condition in the general model).

The model parameters in the calibration activities are set up by considering:

1. only *formcoeff* as variable¸ ranging from 0.1 to 2 (by step of 0.1);
2. constant values for the other parameters, as described in Table 2.

About the use-of-space rules, it is assumed that the individuals could spend 15 hours in contact one to each other, according to the general schedule provided by previous works (Fang et al. 2020). Since the model is based on 15minutes-long simulation step, 60 simulation steps are equal to 1 day. No simulation steps are performed during the night-time (hence, no activity simulated). Besides, it is considered that the individuals could freely move from one part of the cruise to another, by moving for about 50m per step, one at one hour.

[3] all the data are derived by analysing plan schemes reported at https://www.princess.com/ships-and-experience/ships/di-diamond-princess/; last access: 6/4/2020

Parameter	**Value**	**Source**
A	73500m^2 (271 patches per side)	the overall assessed surface area of the cruise from a graphical evaluation (based on the plans[3])
N	3711	(Fang et al. 2020; Mizumoto et al. 2020)
p_{imm}	0 %	no evidence that immune people can exist
Initial infector %	0.054%	considering experimental data (Mizumoto and Chowell 2020), it is calculated as the ratio between 2 observed cases within the median incubation period (Lauer et al. 2020) and N
asymptomatic ratio	20%	the superior limit in the confidence interval of estimated asymptomatic proportion (among all infected cases) (Mizumoto et al. 2020)
average delay	60	equal to 1 day to be shorter than the time to display symptoms (e.g. fever onset) by the 2.5% of infected persons (Fang et al. 2020; Lauer et al. 2020)
Iinc	320	corresponding to the median incubation time (and the inferior limit of the confidence interval), according to a conservative approach. It corresponds to about 5.1 days (Lauer et al. 2020)
Ifev	160	the average value corresponds to the minimum time to display symptoms by the 2.5% of infected persons (Lauer et al. 2020). A standard deviation is associated to make it ranging from 0 to 320 steps.
$prot_i = prot_j$ (*mask filter*)	0	It is considered that all the sample is characterized by the same protection level given by the mask filter, to consider uniform conditions in a conservative approach (Fang et al. 2020). No masks are worn in the calibration simulation (Mizumoto and Chowell 2020; Fang et al. 2020).
t_c	1 step = 15 minutes	consolidated data about closed environment contagion spreading from national and international health organization[1]
mask wearing %	0%	no masks are worn (Mizumoto and Chowell 2020; Fang et al. 2020)
traveled distance	20 patches; 50 patches	two supposed distance between the different main locations in the cruise are tested [3]

Table 2. Model calibration setup: parameters assumed as constant values.

In the calibration activities, simulation is run by using the distinct function in the NLRX package, by assigning 100 seeds for each experiment. Results were collected at every 60 steps in order to take into account the daily dynamics of the process. The number of infected people [pp] per simulation day is evaluated as main comparison output for each sample in the test, and then related average and median values are calculated to be compared to the experimental curve. In particular, the selected *formcoeff* is the one that minimizes the average percentage difference between the infected people assessed by the model median values and the experimental values (Bernardini et al. 2020).

2.3. Application to the case study

The main building in the Faculty of Engineering campus at Università Politecnica delle Marche, Ancona (Italy) has been selected as a significant case study in the university building context. It hosts about 5000 students and professors, who usually attend lessons in classrooms from Monday to Friday, for an overall lessons time of 8 hours per day.

Occupancy issues are characterized by the following main aspects:

- students are divided into course groups, and each group attend the same lessons in different rooms during the day, thus having the possibility to move from a room to another;
- each lesson lasts at least 45 minutes to 1 hour. Afterwards, a lesson break is generally performed, and students generally move towards break areas;
- as a result, contagion spreading connected to occupancy areas considers how classrooms are characterized by main contacts between the same students in a course group, while break areas are affected by possible contacts between different course groups.

Since each students' group is generally considered to attend lessons in the same building area (ideally, the same floor) according to the current scheduling approach, this work does not model the whole main university building, but only a significant part of it (i.e. a single floor of classrooms and breaks areas).

Depending on the case study configuration and on the model calibration activities in Section 2.2, input parameters for the case study simulation are considered as variables (see Table 3) or constant values (see Table 4).

Table 3 gives an overview of the simulation variables assumed as stochastic parameters, described by Probability Density Functions (PDFs).

Parameter	**Min**	**Max**	**PDFs**
N	250	1150	Uniform
Initial infectors %	0.0546	30	Uniform
Mask wearing %	1	100	Uniform
$prot_i = prot_j$ (*mask filter*)	0	1	Uniform
traveled distance	1	100	Uniform

Table 3. Parameter characterization for SA analysis

In particular, the maximum number of initial people *N* has been defined considering the maximum capacity of the classrooms, which corresponds to about 1pp/m^2 inside the classroom. The minimum values consider previously available data of occupancy under different scenarios (i.e. lessons, exams, etc…). *Initial infectors %* has been defined by considering as minimum value the input data for the contagion in the Diamond Princess case study (compare to Section 2.2). A maximum value of 30% of the population is arbitrarily chosen to recreate a possible scenario for local cluster conditions in COVID-19 emergency. *Mask wearing %* has been defined as a uniform probability density function. Finally, mask filter has been defined even as a uniform probability density function, considering that the classification of the masks in groups (i.e. FFPX, KXX) is depending on the ability to stop a specific fraction [0-1] of the aerosol drops, which can affect direct and indirect virus spreading in the adopted proximity-based model.

Concerning the constant parameters, the epidemiological variables are scaled according to the calibration model input set, while *formcoeff* is the best-fitting ones according to calibration results from Section 2.2 activities.

Finally, the overall simulated time is equal to 14 days, which corresponds to 10 days of university opening (320 steps according to Table 4 characterization), because this value can represent a good estimation of the maximum incubation time from previous researches (Lauer et al. 2020) and consolidated data from international health organizations[1]. It can be considered as a critical simulation period since the maximum contagion spread due to the initial infected people has been ideally concluded.

The scenario is firstly assumed to perform a Sensitivity analysis, to understand which are the main independent variables affecting the final results (see Section 2.3.1). Then, the same simulation outputs are compared together depending on such SA results (see Section 2.3.2).

Parameter	**Value**	**Source**
A	4300m^2 (66 patches per side)	the overall assessed surface area of the considered part of the building, by including all the spaces accessible by the students (i.e. classrooms, spaces for study)
formcoeff	Best fitting value according to model calibration activities in Section 2.2	Deriving the spreading phenomenon according to previous experimental data in a closed environment
p_{imm}	0 %	as for the calibration test, since no evidence that immune people can exist
asymptomatic ratio	20%	as for the calibration test
average delay	32	equal to 1 day with 8 hours of attendance by students, by scaling the calibration test parameters
Iinc	170	scaling the calibration test parameters depending on the steps per day length
Ifev	87	scaling the calibration test parameters depending on the steps per day length
t_c	1 step = 15 minutes	consolidated data about closed environment contagion spreading from national and international health organization[1]

Table 4. Case study application: parameters assumed as constant values.

2.3.1. Sensitivity analysis

A Sensitivity Analysis (SA) has been performed through variance-based decomposition (Sobol′ 2001). The Sobol method is used to calculate, for any stochastic input of the performed calculation, total and first-order sensitivity index (STi, SFi). STi (Sobol total index) measures the contribution to the output variance due to each input, including all variance caused by its interactions with any other input variables (Saltelli et al. 2007, 2010). The higher the value of the sensitivity indices, the most influential the respective input on the outcome. SFi measures indicate the main contribution of each input factor to the variance of the output.

Runs were performed using NLRX package (sobol2007 function) of "R statistics" programming language (Salecker et al. 2019), adopting the Sobol variance decomposition scheme proposed by Saltelli (Saltelli et al. 2007, 2010).

After some preliminary tests necessary to improve the accuracy of the proposed model, we performed two sets of 77000 runs according to the aforementioned parameters setting (see Table 3 and Table 4).

2.3.2. Criteria for effectiveness evaluation of mitigation strategies

The results from the simulation scenarios runs performed for Section 2.3.1 are compared together depending on the main independent variables affecting the contagion spreading. Basing on the current solutions in contagion spreading reduction (Fang et al. 2020; Yang et al. 2020; Zhai 2020), results are discussed in terms of:

1. effect of *mask filter* as individuals' protection solution, combined with the *mask wearing %* (classified in homogeneous classes with steps of 10%), that represents the implementation level for the solution. The multiplication between *mask filter* and *mask wearing %* is introduced to have a quick evaluation index combining these two individuals' protection solution-related parameters;
2. *N* as occupancy factors affecting the possibility to implement social distancing solutions. *N* values can be classified according to occupants' density *Docc* [pp/m^2] in classrooms, which are

the occupancy areas. Lower *N*, lower the occupants' density, higher the possibility for the building stakeholders to set up social-distancing solutions inside the world. *Docc* values are offered by 0.1pp/m^2 wide classes. Discretization in 4 density classes is also provide to discuss the effects in relation to the average dimension of the seats in the classrooms: (a) $250 \leq N \leq 350$, $0.2 \text{pp/m}^2 \leq Docc \leq 0.3 \text{pp/m}^2$; (b) $350 < N \leq 600$, $0.3 \text{pp/m}^2 < Docc \leq 0.5 \text{pp/m}^2$; (c) $600 < N \leq 1000$, $0.5 \text{pp/m}^2 < Docc \leq 0.7 \text{pp/m}^2$; (d) $1000 < N \leq 1150$, $0.7 \text{pp/m}^2 < Docc \leq 1.0 \text{pp/m}^2$;

3. *initial infector %* as access control-related factor at the initial simulation step. It is assumed that a good access control solution will detect at least the 95% of the infectors while entering the building starting from the first simulation step. Hence, it is assumed that the implementation of access control strategies will imply *initial infector %* ≤5%; higher values will correspond to no implementation of access control strategies.

These results are organized together to mainly outline different conditions in building operation. As an output, the final infected people percentage *dI* [%] is assessed according to Equation (5)

$$dI = \left[1 - \frac{S_f}{S_{init}}\right] \% \quad (5)$$

where *Sf* [pp] is the final number of susceptible people (not infected) and *Si* [pp] is the initial number of susceptible people (not initially infected). Its trend expresses the contagion spreading within susceptible individuals. Hence, when *dI* tends to 0, all the individuals tend to be not infected while, when *dI* tends to 100%, all the individuals tend to be infected. Solutions effectiveness increases if *dI* is minimized. *dI* values are evaluated at the final simulation step for each considered conditions in the input values, and the distributions of these values are evidenced in respect to the aforementioned input values combinations, by additionally evidencing distribution percentiles. On this distribution, two acceptability limits for the solution effectiveness are selected:

1. *dI*=5%, which implies that at most the 5% of the population will be affected by the virus. This is a conservative limit for the solution effectiveness estimation;

2. *dI*=25%, which implies that at most the 25% of the population will be affected by the virus, according to a quartile analysis of the sample.

Finally, a model resuming the influence of *mask filter*, *mask wearing %* and *Docc* on acceptability limits given by *dI* is proposed to synthetically trace the main simulation results and give a general outlook of the combination between the strategies. To trace such correlation, additional simulation in the range *Docc*=0 to 0.2pp/m2 are performed to represent all the density conditions (also the value under the minimum *N* value considered as acceptable for the university building use).

3. Results

3.1. Model calibration: results

Figure 2 resumes the trend in the number of infected people in the Diamond Princess scenario simulation, by outlining average simulation data for different *formcoeff* values in respect to the experimental data (Mizumoto and Chowell 2020). Infected people are represented by logarithm scale. Data are referred to *traveled distance* equal to 20 patches, but data for 50 patches have the same trend. Higher the *formcoeff*, obviously higher the final number of the infected people. Furthermore, *formcoeff* affect the shape of the contagion curve, according to the following general average trends:

- for *formcoeff* up to 0.2 (dotted lines in Figure 2), the contagion is characterized by an initial peak in the contagion, and then it appears stable, thus evidencing that the higher delay increasing can have significant long term effects (at more than 420 simulation ticks);
- for *formcoeff* from 0.3 to 0.4 (dashed line in Figure 2), the contagion curve has a similar increasing trend as for the experimental curve, but the higher delay increasing slows down the final result;
- for *formcoeff* from 0.5 to 1.4 (continuous black lines in Figure 2), the contagion curve has a similar increasing trend as for the experimental curve, but the predicted values are higher than those of the experimental data. In this sense, the best trend seems to be related to *formcoeff*=0.5, which additionally allows maintaining a conservative approach in infected people's estimation since it is slightly over the experimental curve;

- for *formcoeff* from 1.5 to 2 (continuous grey lines in Figure 2), the contagion curves have a higher peak in respect to the experimental curve (e.g. for *formcoeff*=2, the peak appears at about 360 steps). Hence, the contagion speed is higher, and the peak of infected people is placed before the experimental one, thus increasing short-term contagion effects.

Figure 3 resumes the trend of the best *formcoeff* value (0.5) in fitting the experimental curve. In this condition, the experimental data are placed close to the median values of the 0.5-related curve, with an average percentage error in predictions equal to about 4% in respect to the 50th percentile values (12% in absolute error terms)[4]. Possible differences in the contagion spreading curve are due to specific issues in the cruise use by passengers (e.g. infectors could not "die" in the real scenario; differences in motion schedule).

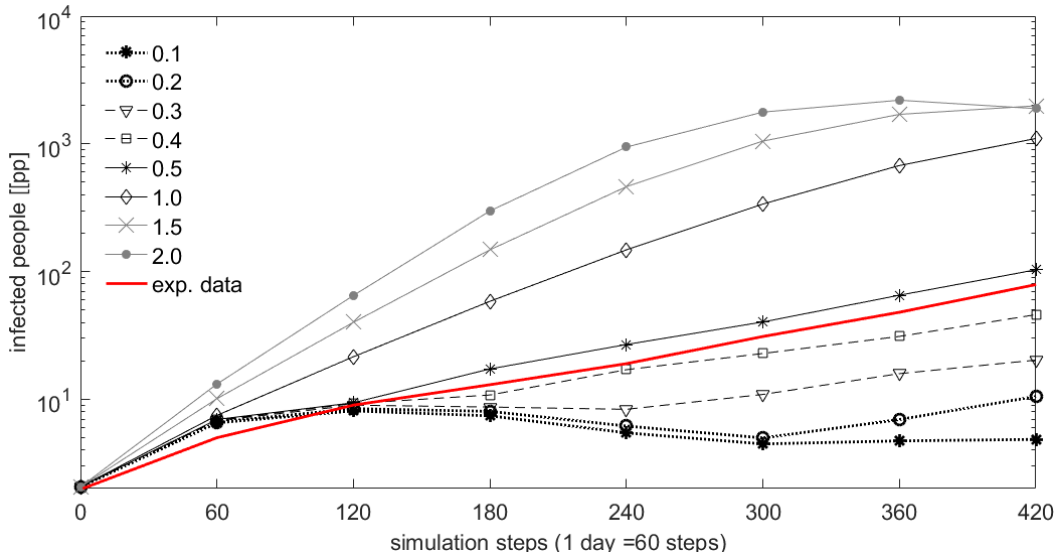

Figure 2. Comparison between the experimental data from the Diamond Princess cruise (red line) and the simulation results, for the main formcoeff values according to their trend. Infected people are represented by logarithm scale.

[4] tests related to 50 patches offer similar outcomes: average percentage error equal to 11%, and in absolute terms equal to 15%

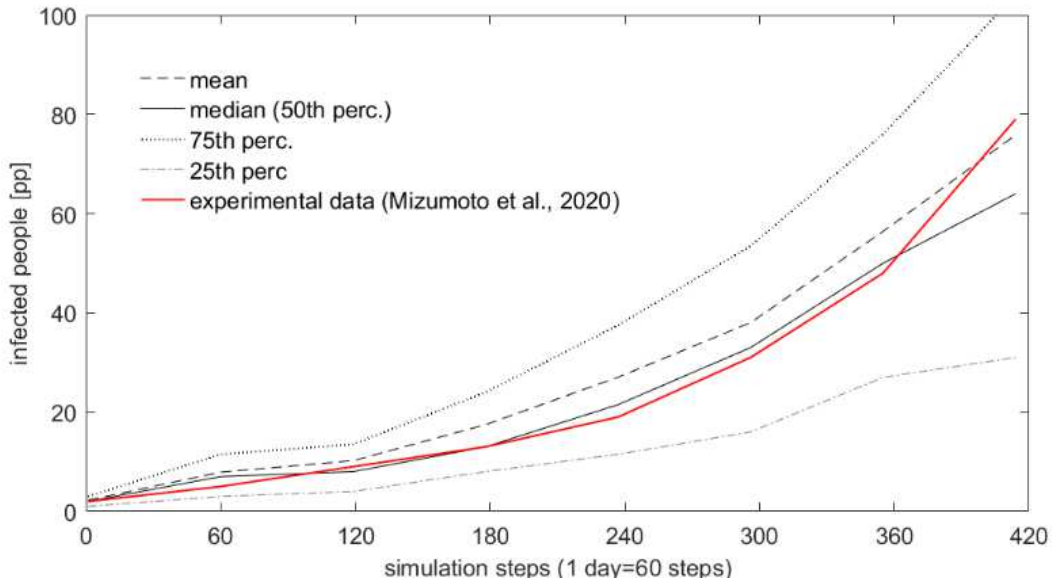

Figure 3. Comparison between the experimental data from the Diamond Princess cruise (red line) and the simulation results, for the best formcoeff values (0.5), by considering different percentiles and mean data.

3.2. Application to the case study: results

According to the results in Section 3.1, all the simulations in the case study are performed by considering *formcoeff*=0.5. In the following sections, the SA results are firstly discussed (Section 3.2.1) and the influence of parameters in the case study are offered (Section 3.2.2).

3.2.1. Sensitivity analysis and robustness check

Figure 4 displays the total order sensitivity indices (STi) and first-order sensitivity indices (SFi).

Considering Total order sensitivity indices (STi), SA suggests that the main source of results' uncertainty is "initial-people" (number of people at the beginning of each simulation run). Considering that spaces where people can move are the same for all the simulations, the value represents the occupation density of the space and also the effect of a possible "social distancing" measure taken to prevent the spread of the contagious disease by maintaining a physical distance between people. The second source of results' uncertainty is *mask filter* (the type of mask adopted in terms of individual protection degree) showing also the importance of individual protection measures.

The other secondary sources of results' uncertainty are *Initial infectors %* and *mask wearing %* previously defined. The effect of *traveled distance* appears negligible.

Considering that the sum of first-order sensitivity indices (SFi) is less than 1 (0.94) the model is non-additive, with limited interactions between input factor, as suggested by (Saltelli et al. 2007).

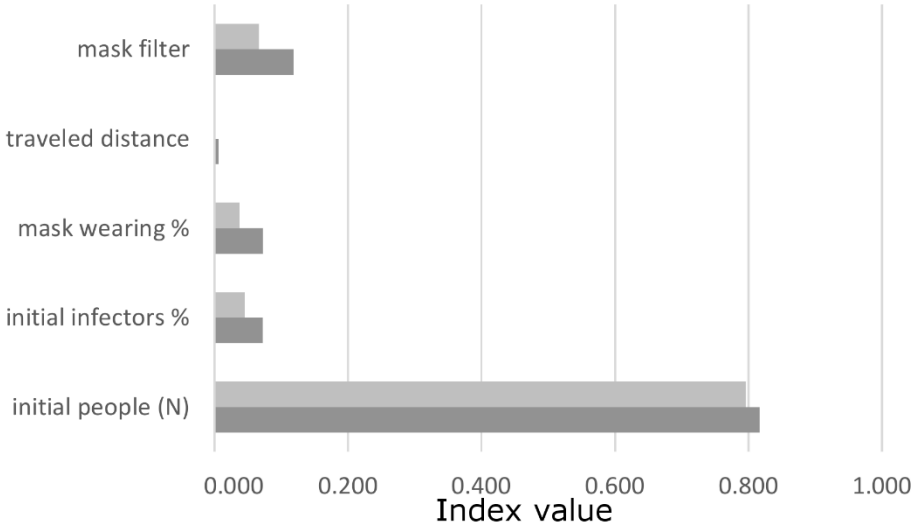

	initial people (N)	initial infectors %	mask wearing %	traveled distance	mask filter
Sobol First Order Index	0.796	0.045	0.038	-	0.066
Sobol Total Order Index	0.817	0.072	0.073	0.006	0.118

Figure 4. Total order sensitivity indices (STi – dark grey) and the first-order sensitivity indices (SFi – light grey) for the considered parameters.

3.2.2. Simulation scenarios results

According to the SA results, the main independent variables are combined to describe different scenarios in the case study. Hence, the effect of the *traveled distance* variable is not here discussed.

3.2.2.1. General influence of the solutions

In general terms, the use of respiratory protective devices with higher *mask filter* values can effectively reduce the virus spreading, especially when the solution is implemented for higher *mask wearing %* values, according to suggestions from previous works (Fang et al. 2020; Zhai 2020). Figure 9Figure 5 resumes the *dI* distribution according to a boxplot representation (no outliers) for

the different *mask filter*mask wearing%* classes, regardless of density-related and access control-related solutions. Higher *mask filter* values implemented by an increasingly higher number of occupants (*mask wearing %* higher values) imply a reduction in the final number of infected occupants. Acceptability thresholds can be reached when implementing at least *mask filter*mask wearing%* ≥*80%* for dI=25% and ≥*0.90%* for dI=5%. Such values essentially imply the necessity to implement at least FFP1 masks (or more protective devices) for at least the 90% of the population.

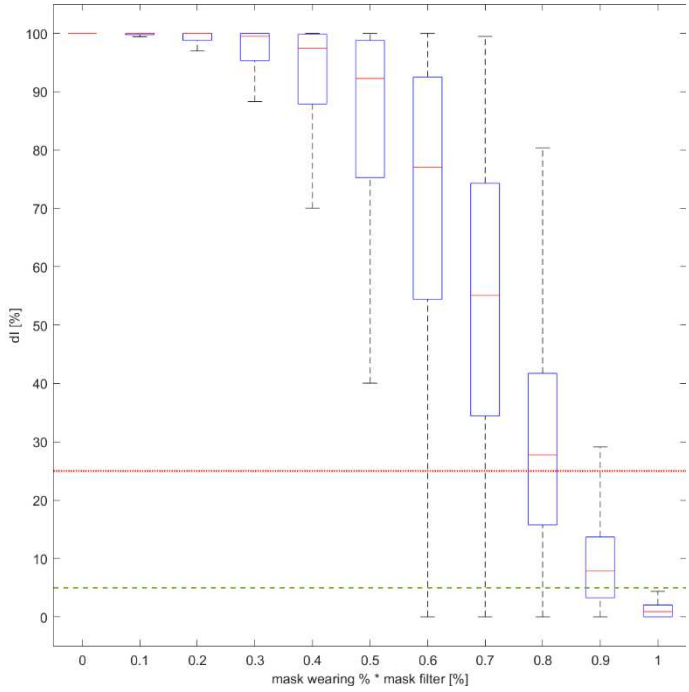

Figure 5. Boxplot dI values distribution at the last simulation step for the whole sample, with respect to the effects related to mask (mask filter and mask wearing %). dI acceptable thresholds are defined at dI=5% (dashed green line) and 25% (continuous red line).

Figure 6 shows how the use of occupants' density control strategies seems to limitedly involve acceptable solutions in terms of *dI* values if applied by themselves. The efficiency of the solution is mainly connected to the possibility to combine such measure to the use of respiratory protective devices, as shown by *Figure 7*. In this sense, the limitation of building use to *Docc*≤0.3pp/m^2 (*Figure 7*-A) allows about a 20% reduction in needed *mask filter*mask wearing%* classes in respect to density maximization conditions (*Figure 7*-D), to obtain dI<25%. Nevertheless, the final result will be affected by the effective possibility to engage users in maintaining social distancing during the whole

occupancy timing. This main reason seems to affect the width of boxplot ranges, especially in *Docc*≤0.3pp/m^2 regardless of additional solutions (see *Figure 6*) and in intermediate conditions in terms of *mask filter*mask wearing%* classes in *Figure 7*.

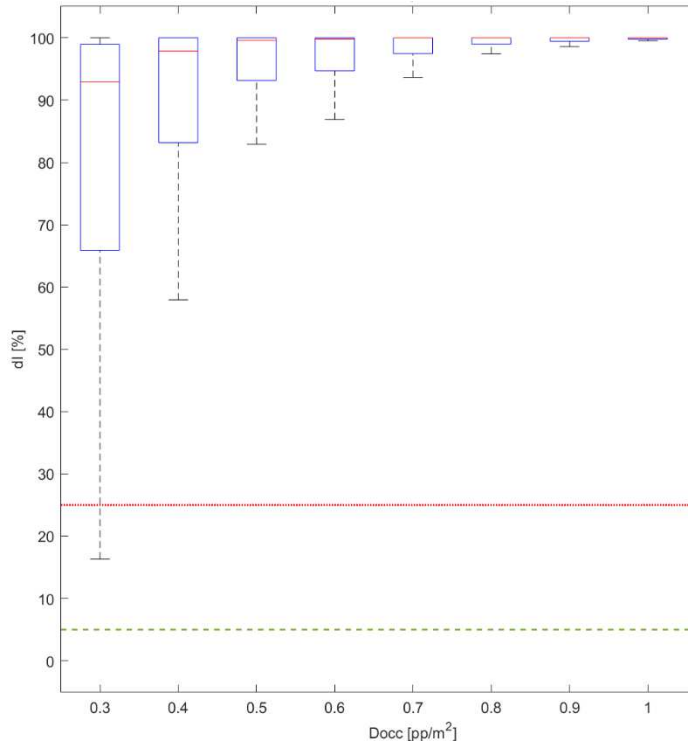

Figure 6. Boxplot dI values distribution at the last simulation step for the whole sample, with respect to the effect of occupants' density Docc values discretized by 0.1pp/m^2. dI acceptable thresholds are defined at dI=5% (dashed green line) and 25% (continuous red line).

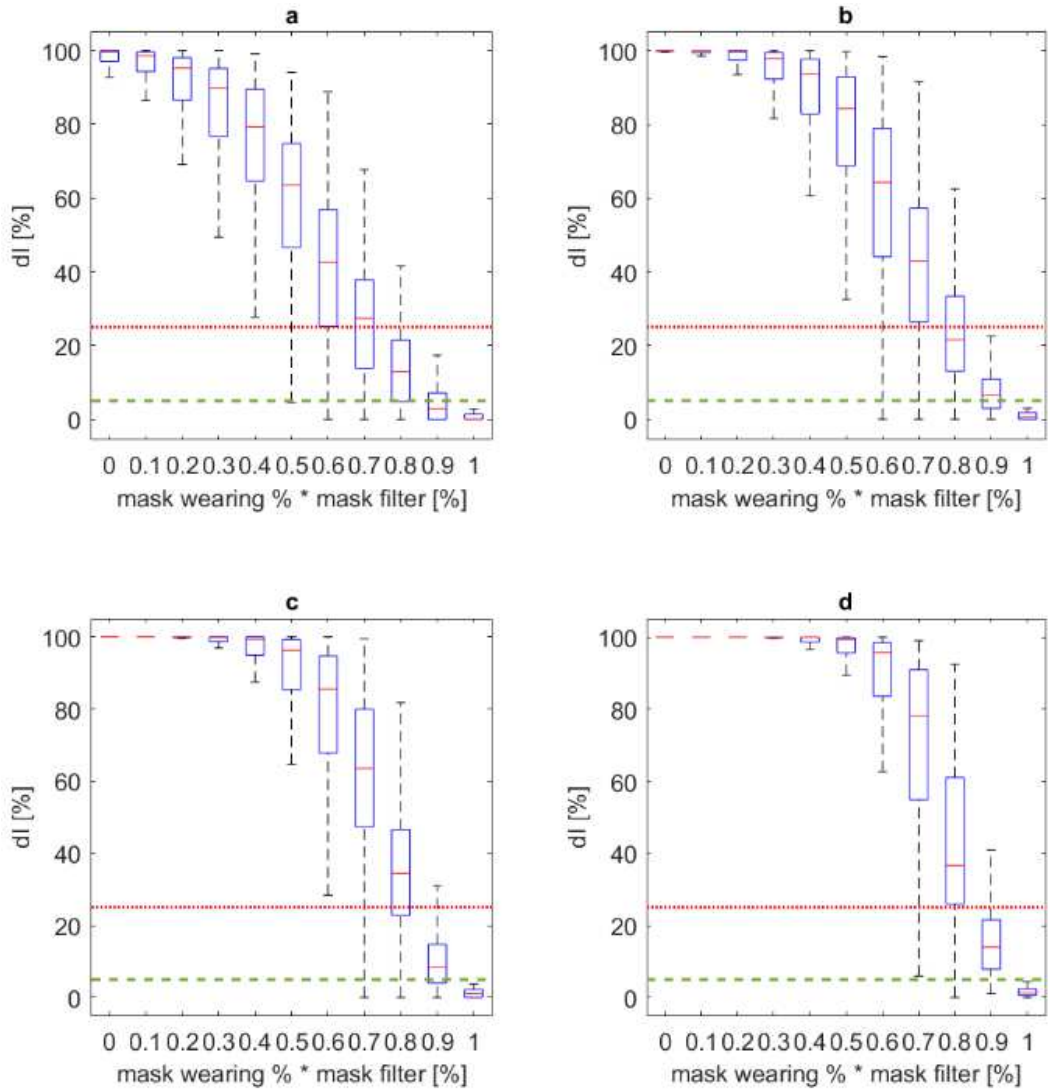

Figure 7. Boxplot dI values distribution at the last simulation step for the whole sample, with respect to the effects of different density classes: a) Docc≤0.3pp/m²; b) 0.3pp/m²<Docc≤0.5pp/m²; c) 0.5pp/m²<Docc≤0.7pp/m²; d) 0.7pp/m²<Docc≤1.0pp/m² . Values are traced according to the overall mask effect. dI acceptable thresholds are defined at dI=5% (dashed green line) and 25% (continuous red line).

Finally, *Figure 8* suggests how the implementation of access control strategies can significantly improve the effect of respiratory protective devices, especially in the case of more consistent solutions. In this sense, the limitation of building access (*Figure 7*-A) allows about 10% reduction in needed *mask filter*mask wearing%* classes in respect to conditions in which no access control are performed, to obtain the outcoming median of dI<5%.

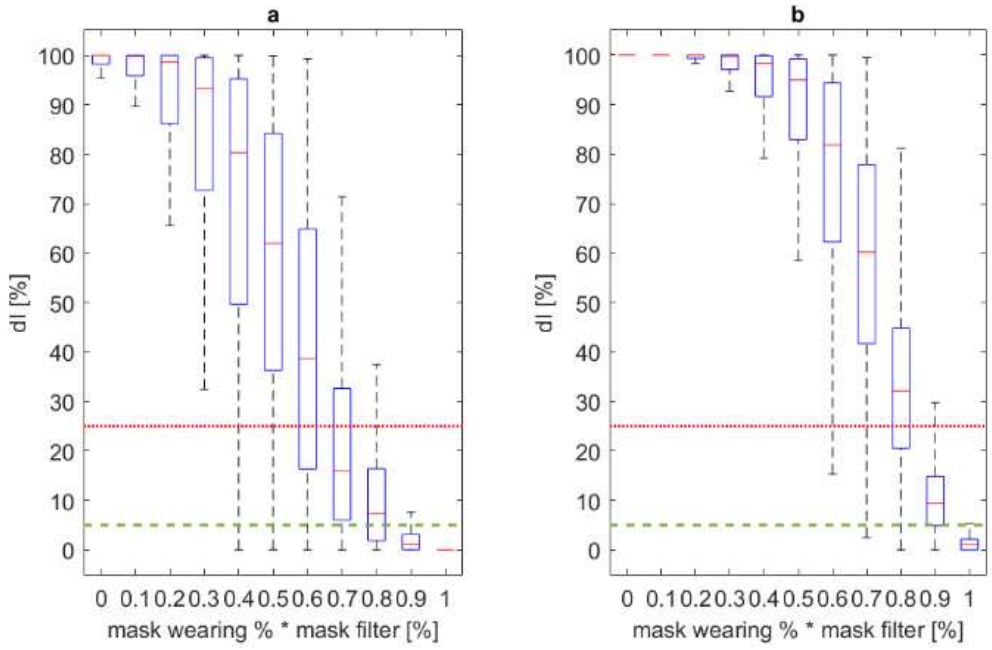

Figure 8. Boxplot dI values distribution at the last simulation step for the whole sample, with respect to: a) access control strategies implemented and b) no access control strategies implemented. Values are traced according to the overall mask effect. dI acceptable thresholds are defined at dI=5% (dashed green line) and 25% (continuous red line).

3.2.2.2. Influence of mask filter at maximum building capacity

According to the general remarks for the whole sample, it could be possible to face maximum building capacity conditions ($0.7pp/m^2<Docc\leq1.0pp/m^2$) by firstly implementing mask filter-based solutions. Figure 9 traces, in the different panels, the effects of mask filter classes on *dI*, depending on the level of implementation within the hosted population (*mask wearing %),* regardless of the access control strategies. The implementation of FFP3 masks for more than 90% of the occupants leads to *dI* values under the *dI* thresholds. The same result is reached in case of no access control strategies implemented, by considering FFP3 and FFP2 implementation, as shown by Figure 10. This outcome is due to the poor effect given by the implementation of access control strategies on the highest mask filter-based solutions, as remarked by *Figure 11*: the main effect given by the implementation of access control strategies is the reduction of the overall dispersion of *dI* data for the class *mask wearing% * mask filter*=80% (see *Figure 11*-A), which is -5% dispersed in respect to the

same class for no access control strategies conditions (see *Figure 11*-B), by considering the interval 25th-75th percentiles. Nevertheless, *Figure 12* shows how poorer mask filter based solutions can take advantages of the access control strategies implementation: in particular, using FFP1 by about the 100% of the population in access control conditions could lead at *dI*<25% for more than the 50% of the simulated cases (*Figure 12*-A; here the FFP1 median at *mask wearing%*=100% is equal to about 10%), while extreme cases for surgical mask implementation falls under the limit dI thresholds(*Figure 12*-B).

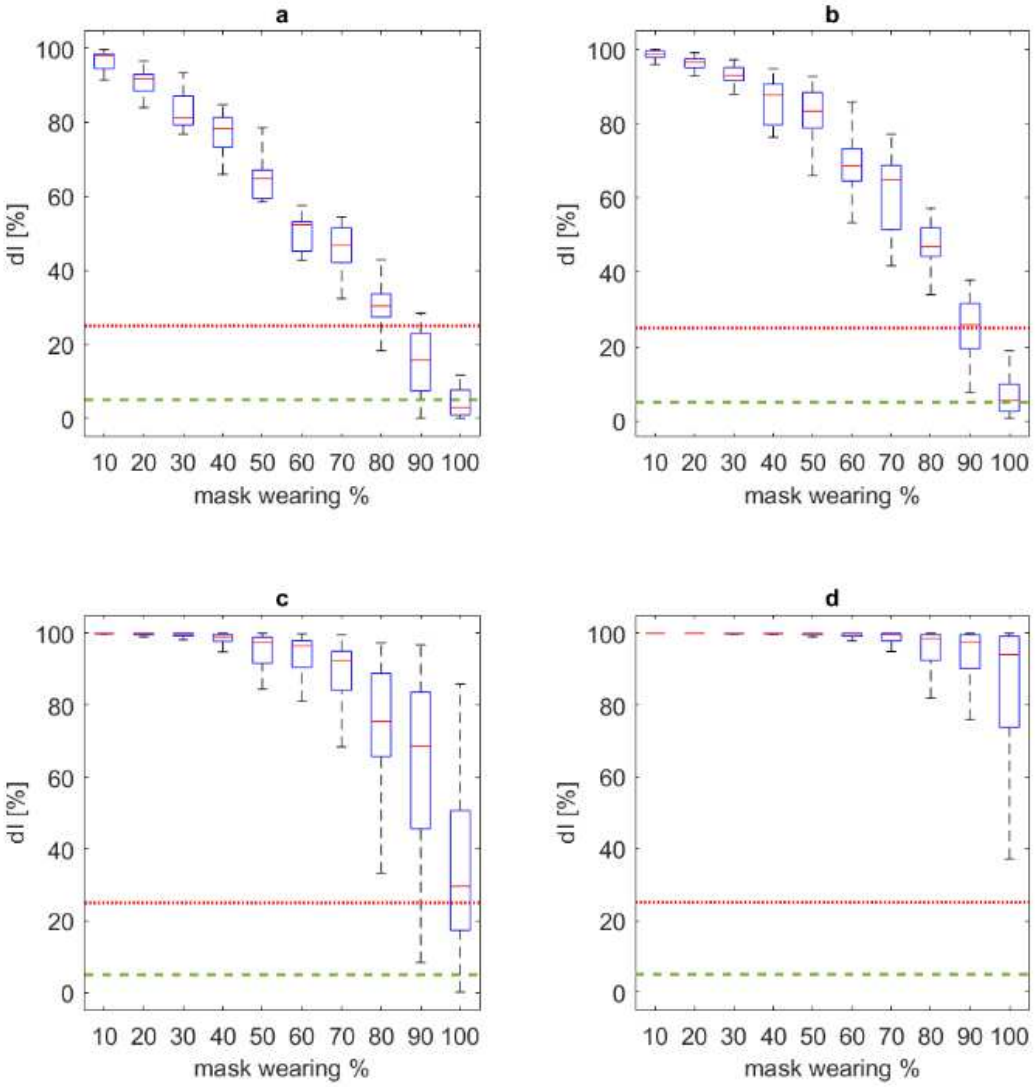

Figure 9. Boxplot dI values distribution at the last simulation step for maximum building capacity, in respect to the effects of different mask filter classes: a) FFP3; b) FFP2; c) FFP1; d) surgical mask.

The Boxplot representation is offered by distinguishing the different mask wearing % classes. dI acceptable thresholds are defined at dI=5% (dashed green line) and 25% (continuous red line).

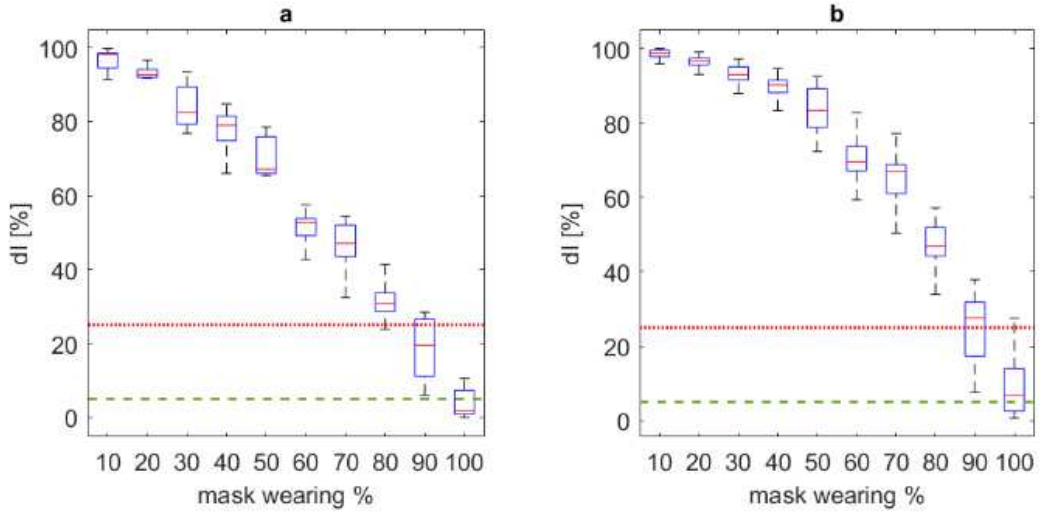

Figure 10. Boxplot dI values distribution at the last simulation step for maximum building capacity in no access control strategies conditions, in respect to the effects of different mask filter classes: a) FFP3; b) FFP2. The Boxplot representation is offered by distinguishing the different mask wearing % classes. dI acceptable thresholds are defined at dI=5% (dashed green line) and 25% (continuous red line).

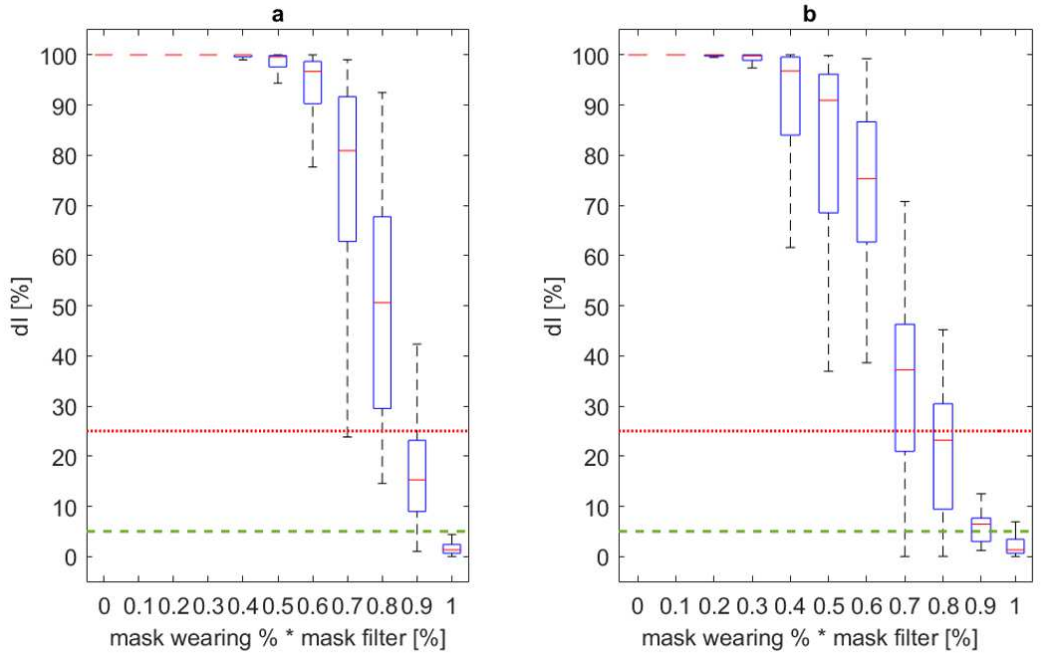

Figure 11. Boxplot dI values distribution at the last simulation step for maximum building capacity, in respect to: a) access control strategies implemented and b) no access control strategies

implemented. Values are traced according to the overall mask effect. dI acceptable thresholds are defined at dI=5% (dashed green line) and 25% (continuous red line).

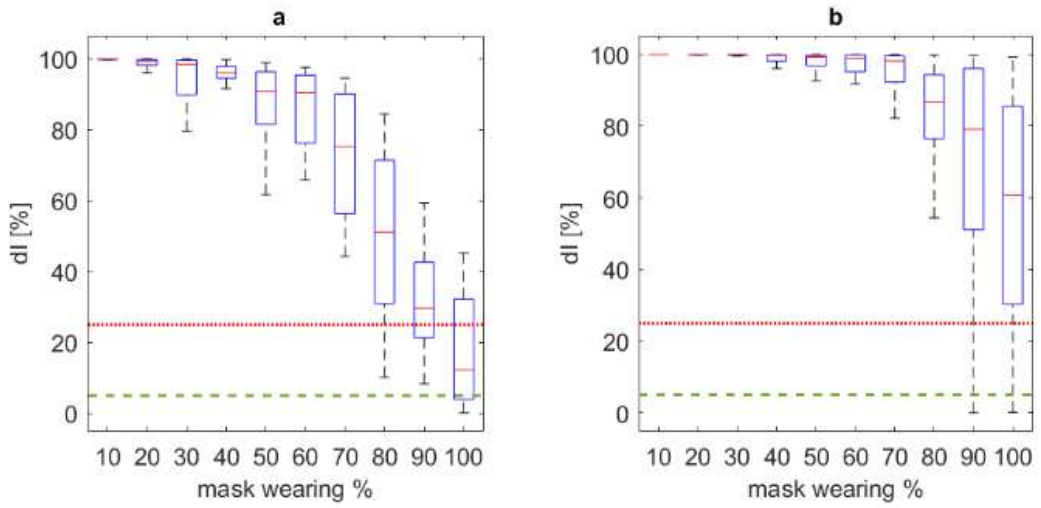

Figure 12. Boxplot dI values distribution at the last simulation step for maximum building capacity when access control strategies are considered, in respect to the effects of different mask filter classes: a) FFP1; b) surgical masks. The Boxplot representation is offered by distinguishing the different mask wearing % classes. dI acceptable thresholds are defined at dI=5% (dashed green line) and 25% (continuous red line).

3.2.2.3. Influence of occupants' density in poor mask-filter based solutions

Figure 13 and Figure 14 shows *dI* distribution values by boxplot representation respectively depending on the adoption of surgical masks and non-standards protection solutions by the users, for scenarios where access control strategies are implemented (Figure 13-B and Figure 14-B) or not (Figure 13-A and Figure 14-A), regardless of the *mask wearing %*. These results shows that:

- a minimum protection level in terms of mask filter should be always guaranteed to the occupants to have limit conditions within the *dI* acceptability thresholds;
- access control strategies in such conditions are always recommended and better benefits can be related to the implementation of occupants' density control.

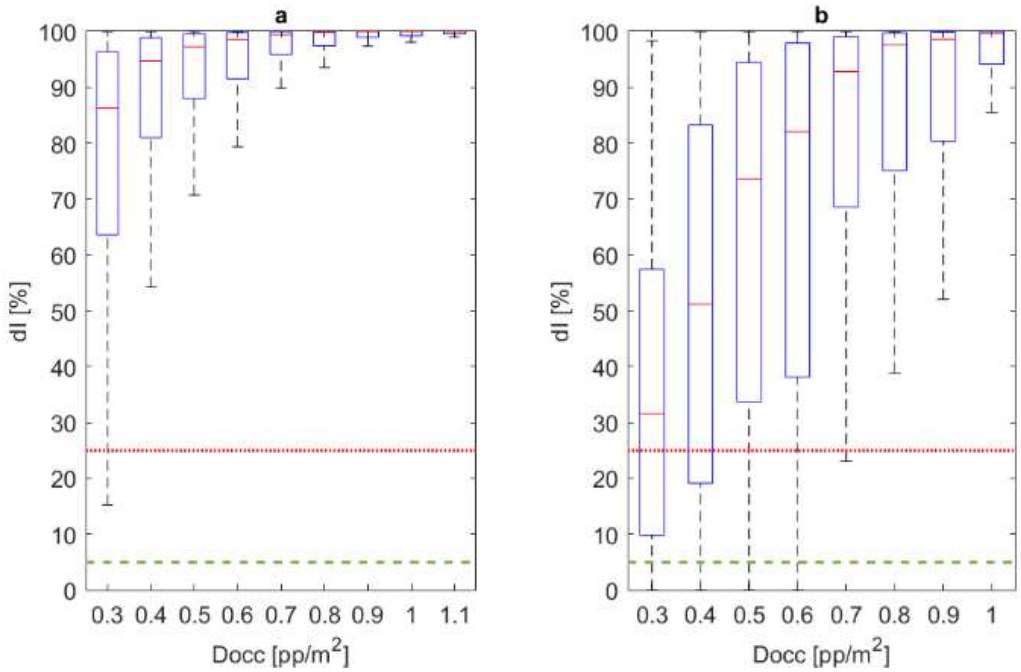

Figure 13. Boxplot dI values distribution at the last simulation step for surgical masks implementation in relation to the occupants' density Docc classes, with respect to: a) no access control strategies implemented; b) access control strategies implemented. Data are offered regardless of the mask wearing % classes. dI acceptable thresholds are defined at dI=5% (dashed green line) and 25% (continuous red line).

The impact of access control strategies is confirmed by *Figure 15*, which demonstrates the impact of *Docc*-related implementation strategies when surgical masks are used by occupants and access control strategies are maintained. A reduction of about 20% in mask wearing % effort could be achieved by passing from 0.5pp/m^2<*Docc*≤0.7pp/m^2 (*Figure 15*-C) to *Docc*≤0.3pp/m^2 (*Figure 15*-A), if considering the dI threshold at 25%. Anyway, *Docc*>0.3pp/m^2 conditions should be avoided, according to *Figure 15*.

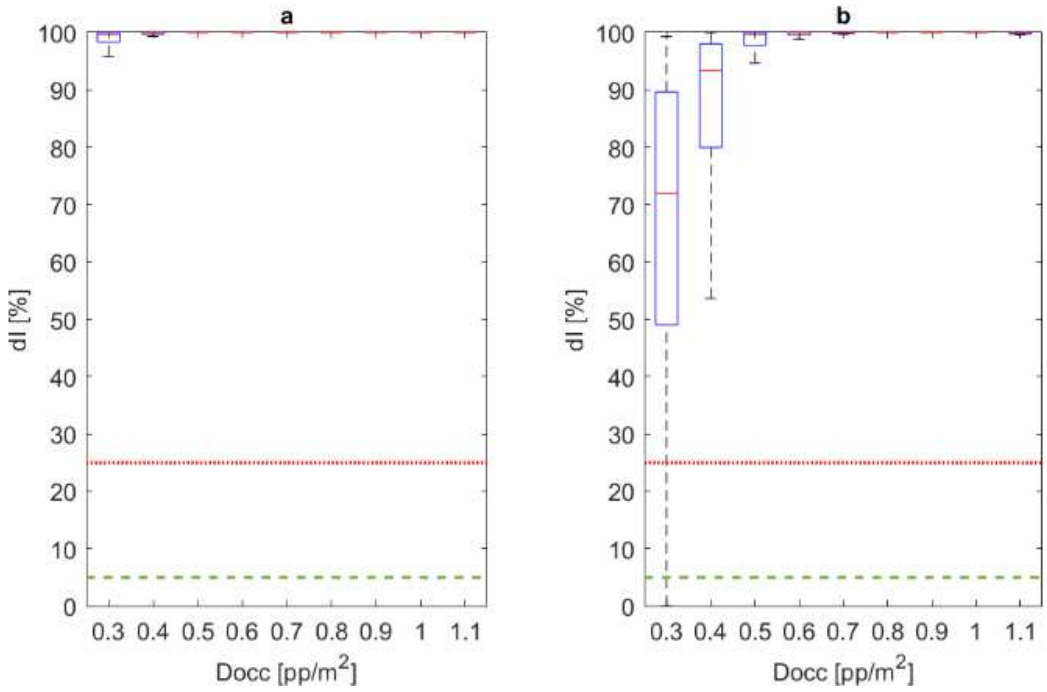

Figure 14. Boxplot dI values distribution at the last simulation step for non-standards protection (0 to 0.25, compare to Table 1) solutions, in relation to the occupants' density Docc classes, with respect to: a) no access control strategies implemented; b) access control strategies implemented. Data are offered regardless of the mask wearing % classes. dI acceptable thresholds are defined at dI=5% (dashed green line) and 25% (continuous red line).

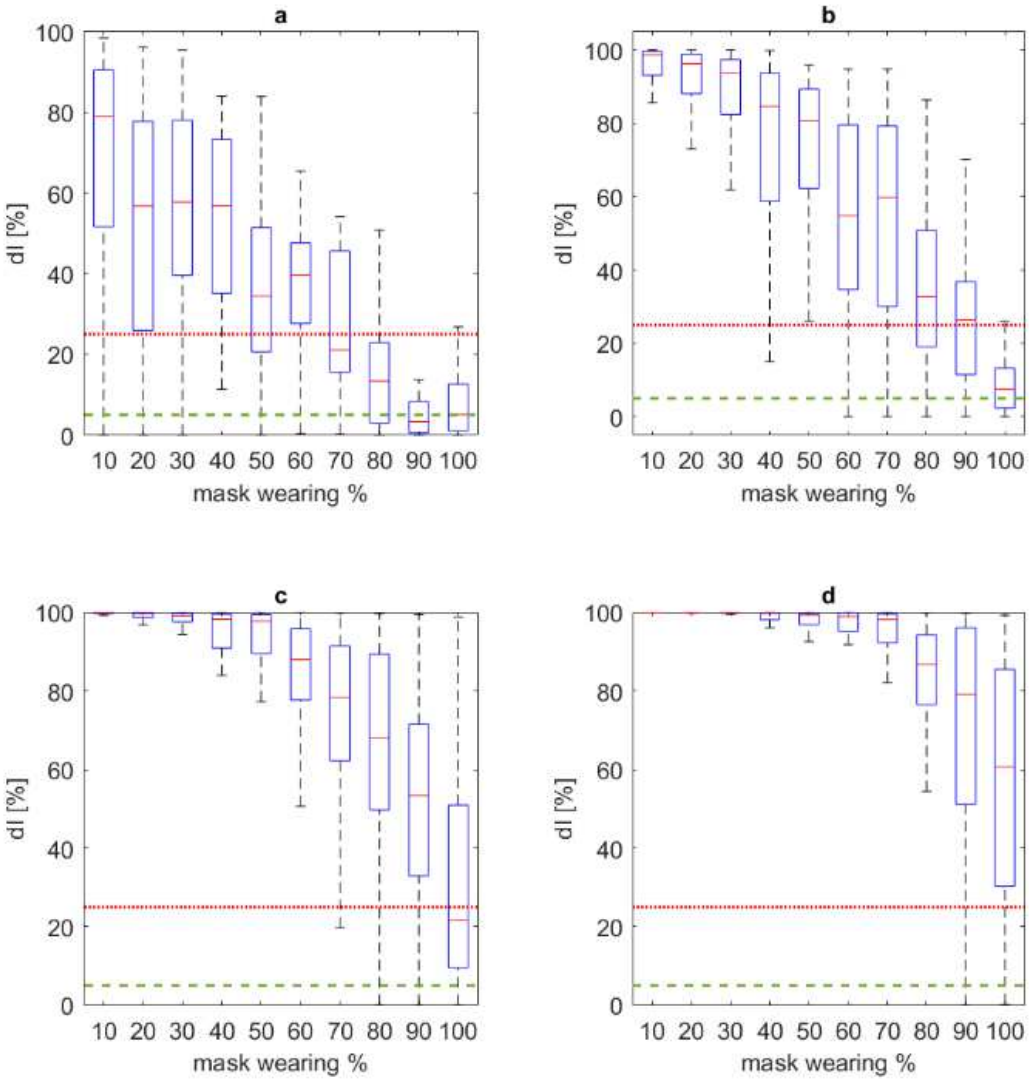

Figure 15. Boxplot dI values distribution at the last simulation step for surgical mask implementation scenarios, with respect to the effects of different density classes: a) Docc≤0.3pp/m²; b) 0.3pp/m²<Docc≤0.5pp/m²; c) 0.5pp/m²<Docc≤0.7pp/m²; d) 0.7pp/m²<Docc≤1.0pp/m² . Values are traced according to the overall mask effect. dI acceptable thresholds are defined at dI=5% (dashed green line) and 25% (continuous red line).

4. Discussion in the view of restart in public buildings and of modelling tools application

Results show the model capabilities in predicting different effects of input conditions due to the university building spaces use (also as relevant example of public building) and to the virus spreading characterization, in the view of the model assumption in Section 1 (i.e. occupancy-based oriented approach for users' simulation and virus spreading; exposure time-based approach according to a

conservative interaction of 15 minutes with possible infected agents; simulation of proximity-based effects on virus transmission in view of a proper Indoor Air Quality control inside the building).

The effective possibility to limit the virus spreading in university buildings could be achieved if only more than 1 risk-reduction solution will be implemented, thus confirming previous works results (Dai and Zhao 2020; Ronchi and Lovreglio 2020).

In general terms, the simulation outcomes evidence how using respiratory protective devices by occupants seems to generally lead to safer conditions for the occupants, especially if high protection measures will be adopted in terms of mask filter ("invasive" masks, like FFP ones) and of widespread implementation (about all the occupants should wear them). The reduction in the building occupants' density could reduce the needed effort in terms of respiratory protective devices especially when access control strategies are implemented to reduce the initial number of infectors entering the building. In this term, the simulation results agree with previous preliminary insights on the importance of facial masks to limit the contagion spreading after the activities restarting (Howard et al. 2020; Zhai 2020). The application of such strategy will lead to move towards the adoption of less invasive masks, e.g. surgical mask, by the whole number of the hosted individuals, as also suggested by review studies (Howard et al. 2020). Such a solution could be more acceptable by the final users.

From a university stakeholder's perspective, the sustainability level depends on the specific aspects involving the strategies:

1. *for mask implementation strategies by the stakeholder*: ensuring that the building occupants (i.e. students and teachers) users should wear facial masks characterized by a specified *mask filter* for at least the considered *mask wearing %* will imply economic (i.e. costs for masks given by the stakeholder) and operational (i.e. activities for distribution of masks to the occupants; staff actions for the control of mask wearing by the occupants) evaluations;
2. *for density control strategies*: the possibility to perform L&T activities with a reduced number of users should be considered depending on the possibility of guaranteeing "remote access" to all the others (i.e. according to the academic continuity perspective and using related remote L&T

tools (Dohaney et al. 2020; Favale et al. 2020)). This aspect should be combined to economic evaluations as well as to the possibility to effectively deploy the measures into the building (e.g. technological access control implementation; use of building staff members at the building entrances; occupants' positioning control solutions), also in relation to facial masks use to increase the occupants' density;

3. *for access control strategies*: deploying staff members or technological solutions to check the users' health state at the entrance should face both economic and operational issues, but also the possibility of guaranteeing rapid access by the users themselves.

Results could be also used to derive simplified rules to combine the strategies together to reach, at most, the acceptable *dI* value. *Figure 16* traces the correlation between *mask filter* values and *Docc* that lead to final simulation results with *dI* placed under the considered acceptability threshold (5% for *Figure 16* -A; 25% for Figure *16*-B), regardless of the *initial infectors %*. The mask filter classes adopted in previous section 3.2.2 are also shown, while the color of data refers to the related mask wearing % values (color bar on the right). Finally, the interpolation of maximum values is offered according to a power-based regression approach (ax^b+c). It is better to evidence that the provided equations just try to give a first rough quantitative measure of the upper boundary limit not to be crossed. This means that no admitted solutions are present over the curve.

The regression shows the limit values for *mask filter values* - *Docc* pairs which can lead to acceptable scenarios according to the defined threshold. Lower values of *mask filter* imply lower values in acceptable densities, also according to Section 3.2.2.3 outcomes. As previously pointed out by Section 3.2.2.2, *Docc* equal to about 1pp/m^2 is admitted only for FFP3 masks implementation.

As expected, maximum pairs and the related regression curves at *dI*=5% are lower than those at *dI*=25%. The general trend and the regression coefficient data confirms simulation results. Some extreme cases could be highlighted by the regression trend. Considering minimum *mask filter* value, *Docc* tends to 0.3pp/m^2 for dI=25%: this density condition essentially refers to the lower cases in the boxplot of Figure 14-B, which refers to the implementation of non-standards protection solutions in

combination with access control strategies. Regression predictions move closer for FFP2 and FFP3 mask implementation. Finally, 95% of confidence intervals regression curves evidence possible upper and lower bounds of the models. In case of a more conservative approach, it should better use the lowest dashed curves (lower confidence bond at 2.5%), which essentially admit as an acceptable solution the adoption of surgical masks at the lowest densities (e.g.: for dI=5%: for Docc ranging from 0.0 to 0.1pp/m^2, the *mask filter* is close to 0.54).

Since the model does not include the *mask wearing %* as prediction input, the proposed regression model can be adopted also when the users wear respiratory protective devices with different *mask filter* values, by conservatively considering that the *mask filter* to be considered will be the one of the lower one. Furthermore, the *mask wearing %* data on Figure 16 outline the minimum values for the pair implementation.

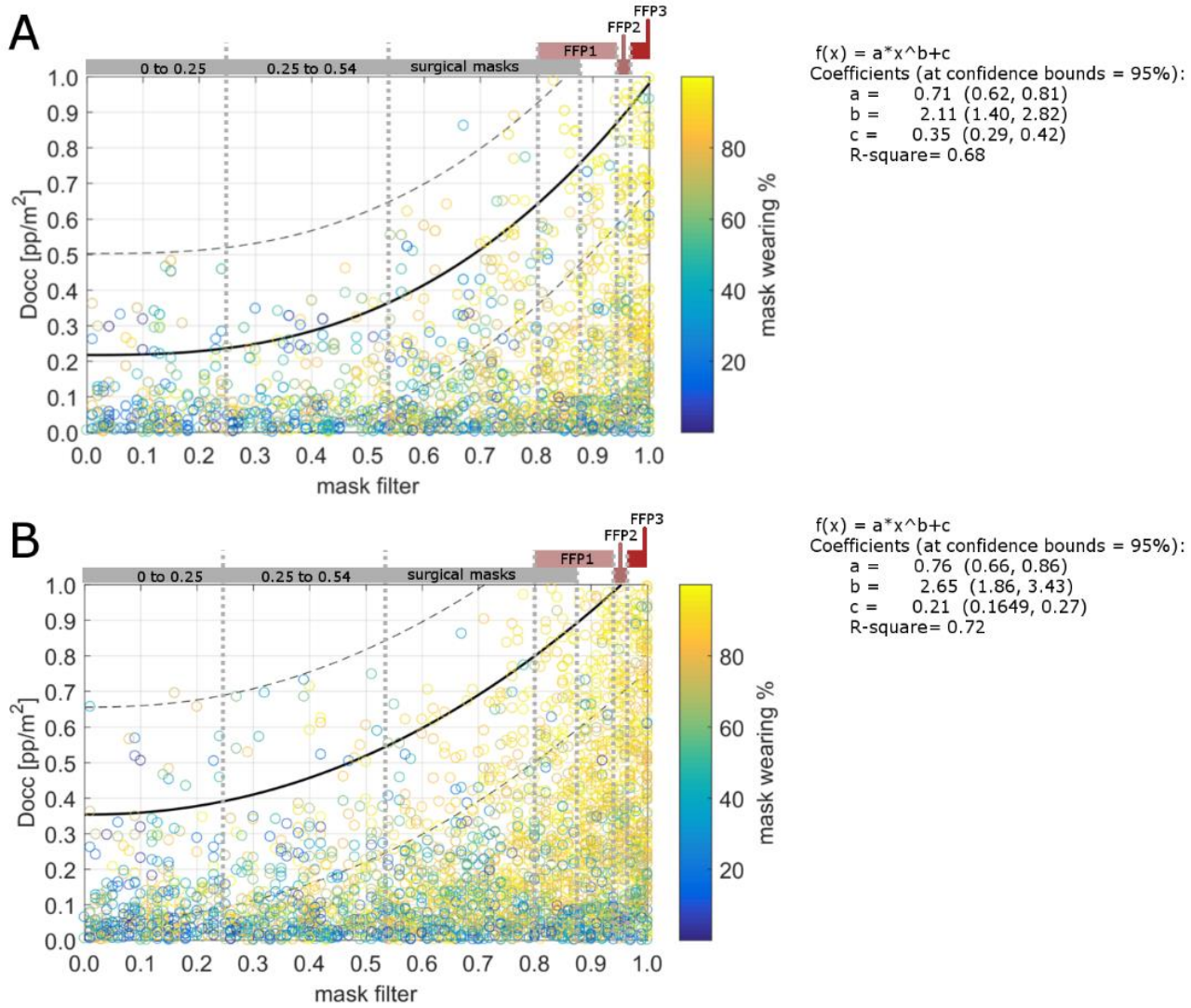

Figure 16. Mask filter-Docc correlation for all the pairs related to a) dI≤5% and b) dI≤25%. The pairs' colour is related to the mask wearing %. Regression curves (ax^b+c) are shown by providing 95% of confidence intervals regression (dashed lines; see equation coefficients on the right of each panel). Mask filter classes are also shown in the upper part of the graphs.

From a modelling perspective, results confirm how the developed simulator could effectively represent different scenarios in university buildings depending on the input factors used to estimate the virus spreading probability. The calibration of the model is performed from current available experimental data, to reproduce real-world conditions in the simulated environment. When other data will be available, it will be possible to update such calibration, by also including, for example, additional modes of person-to-person transmission means or person-to-building components (i.e., contact with contaminated objects) or systems (e.g. ventilation systems) (Noakes and Sleigh 2009; Pica and Bouvier 2012; Emmerich et al. 2013; Gao et al. 2016; Adams et al. 2016; Zhang et al. 2018).

Besides, specification on the layout in terms of geometry and presence of obstacles could be implemented, to better take into account the additional architectural features affecting the virus spreading according to consolidate literature on airborne diseases (Pica and Bouvier 2012; Prussin et al. 2020).

Finally, the model considers the possibility to have "new" infected individuals only inside the building. This aspect could effectively represent most of the basic conditions in the return to "business as usual" in which the agents' life does not include the participation to social activities and limit "unsafe" contacts outside of the "working" (or "studying") places. Anyway, the daily infector percentage in the model could vary if considering additional new infected people/infectors whose contagion happened outside of the building.

5. Conclusions

The COVID-19 event evidences how simulation tools could be adopted by building decision makers to evaluate how different risk-mitigation strategies for the safety of occupants against a pandemic could guarantee adequate levels of reliability and feasibility for both the stakeholders and

the end users. In fact, simulators can be used to optimize the measures against secondary virus outbreaks among the communities while maintaining adequate conditions for the fruition and use of the closed environment itself. In this general context, decision makers of university buildings could take advantage of these tools in the view to avoid further academic disruption in such relevant kind of public buildings.

This paper provides the development of an agent-based model to estimate the impact of different risk-mitigation strategies virus spreading in university buildings by considering consolidate proximity-based and exposure time-based rules given by international health organizations. A probabilistic approach is adopted to this end, by mainly focusing on the representation of occupancy issues in main areas for university Learning and Teaching (L&T) activities (i.e. classrooms and break areas) , according to the related schedule, and the presence of the same "day-to-day" users (i.e. students and teachers). The model can also include the representation of contagion-mitigation strategies connected to the use of facial masks/respiratory protective devices, occupants' density control (in the view of maintaining social-distancing strategies) and other access control strategies. It is also able to provide a first quantitative measure of the implementation of such strategies by the relative stakeholders. After its implementation in a software tool and the calibration activities (through available experimental data in a closed environment), the simulator is applied to a significant university case study

Besides the possibility to reproduce what happened in such a COVID-19-affected closed environment, results show how the model can represent the impact of the contagion-mitigation strategies during the time. Hence, the effectiveness of each strategy (as individually adopted) and of the combination between different measures could be evaluated by the simulator.

In the considered university case study, results show that the major effectiveness seems to be reachable by using respiratory protective devices (i.e. FFPk masks), regardless of the implementation of other strategies. Nevertheless, the adoption of FFPk devices can generally imply a low level of acceptability by the users, since they are not comfortable and easy-to-use by non-specialized users.

An acceptable level of effectiveness could be reached by combining different measures, i.e. the use of facial masks and the control of occupants' densities. Limiting the number of people inside the application building could support the implementation of surgical masks by the users, thus improving the mask-related operational conditions for the occupants. According to the results for the case study application evidence, the occupants' density for users wearing surgical masks should be at most halved to reach the same effectiveness of full occupants' density with FFP3 mask worn. By this way, the effects of L&T activities disruption and limitation could be majorly avoided, but the organization of activities in a "mixed" way (presence of some users plus remote access for the others) should be encouraged. The stakeholders could support operational decisions by the model, according to both cost-benefits and users' acceptability standpoints. Similar criteria could be extended to other kinds of public buildings, by considering their building intended-use peculiarities.

The model is based on some main assumptions related to consolidated transmission modes (i.e. proximity-based and exposure time-based, by avoiding to consider aerosol-related issues), simplified representation of building (according to area-based approaches instead of representing each layout element) and the introduction in the simulation scenario of multiple "attraction areas" or occupancy schedule features (in the university: classrooms and break areas). Although the combination between such factors could affect the results about specific scenarios, the probabilistic approach moves towards the definition of general outcomes based on the different input scenario which can appear in the public building spaces (i.e. in the university, as in the case study), thanking to the simulation-based statistics.

The model is a preliminary and easy-to-apply model which could increase the risk-awareness for decision-makers, and calibration and case study application results evidence its capabilities. Furthermore, thanks to the adopted approach (i.e. agent-based modelling techniques), the model could be easily modified to integrate such aspects in future researches, by also focusing on different epidemiological data (including modes of virus transmission), different build environment and building intended use with similar activities scheduling and occupancy tasks (e.g.: public buildings;

modification to include layout features), with the final perspective to apply it to different relevant contexts characterized by long-lasting occupants' presence in some main areas, such as tourist facilities, cultural buildings and so on.

Declarations of interest: none

6. References

Adams RI, Bhangar S, Dannemiller KC, et al (2016) Ten questions concerning the microbiomes of buildings. Building and Environment 109:224–234. https://doi.org/10.1016/j.buildenv.2016.09.001

Anderson RM, Heesterbeek H, Klinkenberg D, Hollingsworth TD (2020) How will country-based mitigation measures influence the course of the COVID-19 epidemic? The Lancet 395:931–934. https://doi.org/10.1016/S0140-6736(20)30567-5

Azimi P, Keshavarz Z, Cedeno Laurent JG, et al (2020) Mechanistic Transmission Modeling of COVID-19 on the Diamond Princess Cruise Ship Demonstrates the Importance of Aerosol Transmission. medRxiv 2020.07.13.20153049. https://doi.org/10.1101/2020.07.13.20153049

Banos A, Lang C, Marilleau N (2015) Agent-Based Spatial Simulation with NetLogo

Bernardini G, Quagliarini E, D'Orazio M, Brocchini M (2020) Towards the simulation of flood evacuation in urban scenarios: Experiments to estimate human motion speed in floodwaters. Safety Science 123:104563. https://doi.org/10.1016/j.ssci.2019.104563

Bruinen de Bruin Y, Lequarre A-S, McCourt J, et al (2020) Initial impacts of global risk mitigation measures taken during the combatting of the COVID-19 pandemic. Safety Science 128:104773. https://doi.org/10.1016/j.ssci.2020.104773

Casareale C, Bernardini G, Bartolucci A, et al (2017) Cruise ships like buildings: Wayfinding solutions to improve emergency evacuation. Building Simulation 10:989–1003. https://doi.org/10.1007/s12273-017-0381-0

Chen C, Xu L, Zhao D, et al (2020) A new model for describing the urban resilience considering adaptability, resistance and recovery. Safety Science 128:104756. https://doi.org/10.1016/j.ssci.2020.104756

Cirrincione L, Plescia F, Ledda C, et al (2020) COVID-19 Pandemic: Prevention and Protection Measures to Be Adopted at the Workplace. Sustainability 12:3603. https://doi.org/10.3390/su12093603

D'Orazio M, Quagliarini E, Bernardini G, Spalazzi L (2014) EPES - Earthquake pedestrians' evacuation simulator: A tool for predicting earthquake pedestrians' evacuation in urban outdoor scenarios. International Journal of Disaster Risk Reduction 10:153–177. https://doi.org/10.1016/j.ijdrr.2014.08.002

Dai H, Zhao B (2020) Association of the infection probability of COVID-19 with ventilation rates in confined spaces. Building Simulation. https://doi.org/10.1007/s12273-020-0703-5

Dohaney J, de Roiste M, Salmon RA, Sutherland K (2020) Benefits, barriers, and incentives for improved resilience to disruption in university teaching. International Journal of Disaster Risk Reduction 101691. https://doi.org/10.1016/j.ijdrr.2020.101691

Dong B, Yan D, Li Z, et al (2018) Modeling occupancy and behavior for better building design and operation—A critical review. Building Simulation 11:899–921. https://doi.org/10.1007/s12273-018-0452-x

Emmerich SJ, Heinzerling D, Choi J, Persily AK (2013) Multizone modeling of strategies to reduce the spread of airborne infectious agents in healthcare facilities. Building and Environment 60:105–115. https://doi.org/10.1016/j.buildenv.2012.11.013

Fanelli D, Piazza F (2020) Analysis and forecast of COVID-19 spreading in China, Italy and France. Chaos, Solitons & Fractals 134:109761. https://doi.org/10.1016/j.chaos.2020.109761

Fang Z, Huang Z, Li X, et al (2020) How many infections of COVID-19 there will be in the "Diamond Princess"-Predicted by a virus transmission model based on the simulation of crowd flow

Favale T, Soro F, Trevisan M, et al (2020) Campus traffic and e-Learning during COVID-19 pandemic. Computer Networks 176:107290. https://doi.org/10.1016/j.comnet.2020.107290

Gao N, Niu J, Morawska L (2008) Distribution of respiratory droplets in enclosed environments under different air distribution methods. Building Simulation 1:326–335. https://doi.org/10.1007/s12273-008-8328-0

Gao X, Wei J, Lei H, et al (2016) Building Ventilation as an Effective Disease Intervention Strategy in a Dense Indoor Contact Network in an Ideal City. PLOS ONE 11:e0162481. https://doi.org/10.1371/journal.pone.0162481

Howard J, Huang A, Li Z, et al (2020) Face Masks Against COVID-19: An Evidence Review. Preprints 2020040203:. https://doi.org/10.20944/preprints202004.0203.v1

Laskowski M, Demianyk BCP, Witt J, et al (2011) Agent-Based Modeling of the Spread of Influenza-Like Illness in an

Emergency Department: A Simulation Study. IEEE Transactions on Information Technology in Biomedicine 15:877–889. https://doi.org/10.1109/TITB.2011.2163414

Lauer SA, Grantz KH, Bi Q, et al (2020) The Incubation Period of Coronavirus Disease 2019 (COVID-19) From Publicly Reported Confirmed Cases: Estimation and Application. Annals of Internal Medicine. https://doi.org/10.7326/M20-0504

Lopez LR, Rodo X (2020) A modified SEIR model to predict the COVID-19 outbreak in Spain and Italy: simulating control scenarios and multi-scale epidemics. (preprint on www.medrxiv.org). https://doi.org/10.1101/2020.03.27.20045005

Mizumoto K, Chowell G (2020) Transmission potential of the novel coronavirus (COVID-19) onboard the diamond Princess Cruises Ship, 2020. Infectious Disease Modelling 5:264–270. https://doi.org/10.1016/j.idm.2020.02.003

Mizumoto K, Kagaya K, Zarebski A, Chowell G (2020) Estimating the asymptomatic proportion of coronavirus disease 2019 (COVID-19) cases on board the Diamond Princess cruise ship, Yokohama, Japan, 2020. Eurosurveillance 25:. https://doi.org/10.2807/1560-7917.ES.2020.25.10.2000180

Murray OM, Bisset JM, Gilligan PJ, et al (2020) Respirators and surgical facemasks for COVID-19: implications for MRI. Clinical Radiology. https://doi.org/10.1016/j.crad.2020.03.029

Noakes CJ, Sleigh PA (2009) Mathematical models for assessing the role of airflow on the risk of airborne infection in hospital wards. Journal of The Royal Society Interface 6:. https://doi.org/10.1098/rsif.2009.0305.focus

Pica N, Bouvier NM (2012) Environmental factors affecting the transmission of respiratory viruses. Current Opinion in Virology 2:90–95. https://doi.org/10.1016/j.coviro.2011.12.003

Prem K, Liu Y, Russell TW, et al (2020) The effect of control strategies to reduce social mixing on outcomes of the COVID-19 epidemic in Wuhan, China: a modelling study. The Lancet Public Health. https://doi.org/10.1016/S2468-2667(20)30073-6

Prussin AJ, Belser JA, Bischoff W, et al (2020) Viruses in the Built Environment (VIBE) meeting report. Microbiome 8:1. https://doi.org/10.1186/s40168-019-0777-4

Rengasamy S, Shaffer R, Williams B, Smit S (2017) A comparison of facemask and respirator filtration test methods. Journal of Occupational and Environmental Hygiene 14:92–103. https://doi.org/10.1080/15459624.2016.1225157

Ronchi E, Lovreglio R (2020) EXPOSED: An occupant exposure model for confined spaces to retrofit crowd models during a pandemic. Safety Science 130:104834. https://doi.org/10.1016/j.ssci.2020.104834

Saari A, Tissari T, Valkama E, Seppänen O (2006) The effect of a redesigned floor plan, occupant density and the quality of indoor climate on the cost of space, productivity and sick leave in an office building–A case study. Building and Environment 41:1961–1972. https://doi.org/10.1016/j.buildenv.2005.07.012

Salecker J, Sciaini M, Meyer KM, Wiegand K (2019) The nlrx r package: A next-generation framework for reproducible NetLogo model analyses. Methods in Ecology and Evolution 10:1854–1863. https://doi.org/10.1111/2041-210X.13286

Saltelli A, Annoni P, Azzini I, et al (2010) Variance based sensitivity analysis of model output. Design and estimator for the total sensitivity index. Computer Physics Communications 181:259–270. https://doi.org/10.1016/j.cpc.2009.09.018

Saltelli A, Ratto M, Andres T, et al (2007) Global Sensitivity Analysis. The Primer. John Wiley & Sons, Ltd, Chichester, UK

Servick K (2020) Cellphone tracking could help stem the spread of coronavirus. Is privacy the price? Science. https://doi.org/10.1126/science.abb8296

Shiina A, Niitsu T, Kobori O, et al (2020) Relationship between perception and anxiety about COVID-19 infection and risk behaviors for spreading infection: A national survey in Japan. Brain, Behavior, & Immunity - Health 6:100101. https://doi.org/10.1016/j.bbih.2020.100101

Sobol′ I. (2001) Global sensitivity indices for nonlinear mathematical models and their Monte Carlo estimates. Mathematics and Computers in Simulation 55:271–280. https://doi.org/10.1016/S0378-4754(00)00270-6

Wang H, Qian H, Zhou R, Zheng X (2020) A novel circulated air curtain system to confine the transmission of exhaled contaminants: A numerical and experimental investigation. Building Simulation. https://doi.org/10.1007/s12273-020-0667-5

Wilder-Smith A, Chiew CJ, Lee VJ (2020) Can we contain the COVID-19 outbreak with the same measures as for SARS? The Lancet Infectious Diseases. https://doi.org/10.1016/S1473-3099(20)30129-8

Wilensky U (1999) NetLogo. http://ccl.northwestern.edu/netlogo/. In: Center for Connected Learning and Computer-Based Modeling, Northwestern University, Evanston, IL

Yang Y, Peng F, Wang R, et al (2020) The deadly coronaviruses: The 2003 SARS pandemic and the 2020 novel coronavirus epidemic in China. Journal of Autoimmunity 102434. https://doi.org/10.1016/j.jaut.2020.102434

Zhai Z (2020) Facial mask: A necessity to beat COVID-19. Building and Environment 175:106827. https://doi.org/10.1016/j.buildenv.2020.106827

Zhang N, Huang H, Su B, et al (2018) A human behavior integrated hierarchical model of airborne disease transmission in a large city. Building and Environment 127:211–220. https://doi.org/10.1016/j.buildenv.2017.11.011

Zheng X, Zhong T, Liu M (2009) Modeling crowd evacuation of a building based on seven methodological approaches. Building and Environment 44:437–445. https://doi.org/10.1016/j.buildenv.2008.04.002

Zizzo M, Bollino R, Castro Ruiz C, et al (2020) Surgical management of suspected or confirmed SARS-CoV-2 (COVID-19)-positive patients: a model stemming from the experience at Level III Hospital in Emilia-Romagna, Italy. European Journal of Trauma and Emergency Surgery 46:513–517. https://doi.org/10.1007/s00068-020-01377-2

Figures

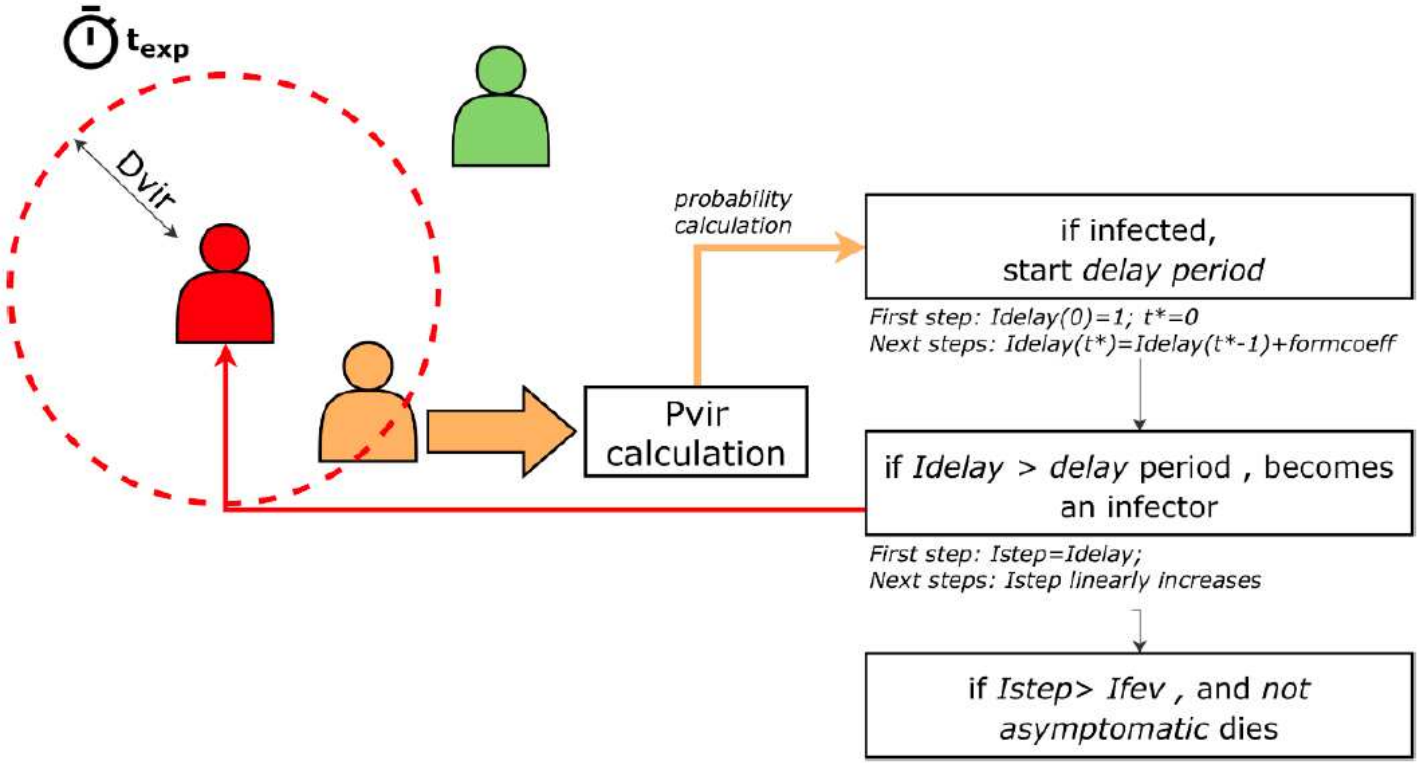

Figure 1

General scheme for the contagion spreading: the red agent is an infector, the green agent is out of Dvir, the orange agent is a possible infected agent. The Pvir calculation also depends on the exposure timing texp.

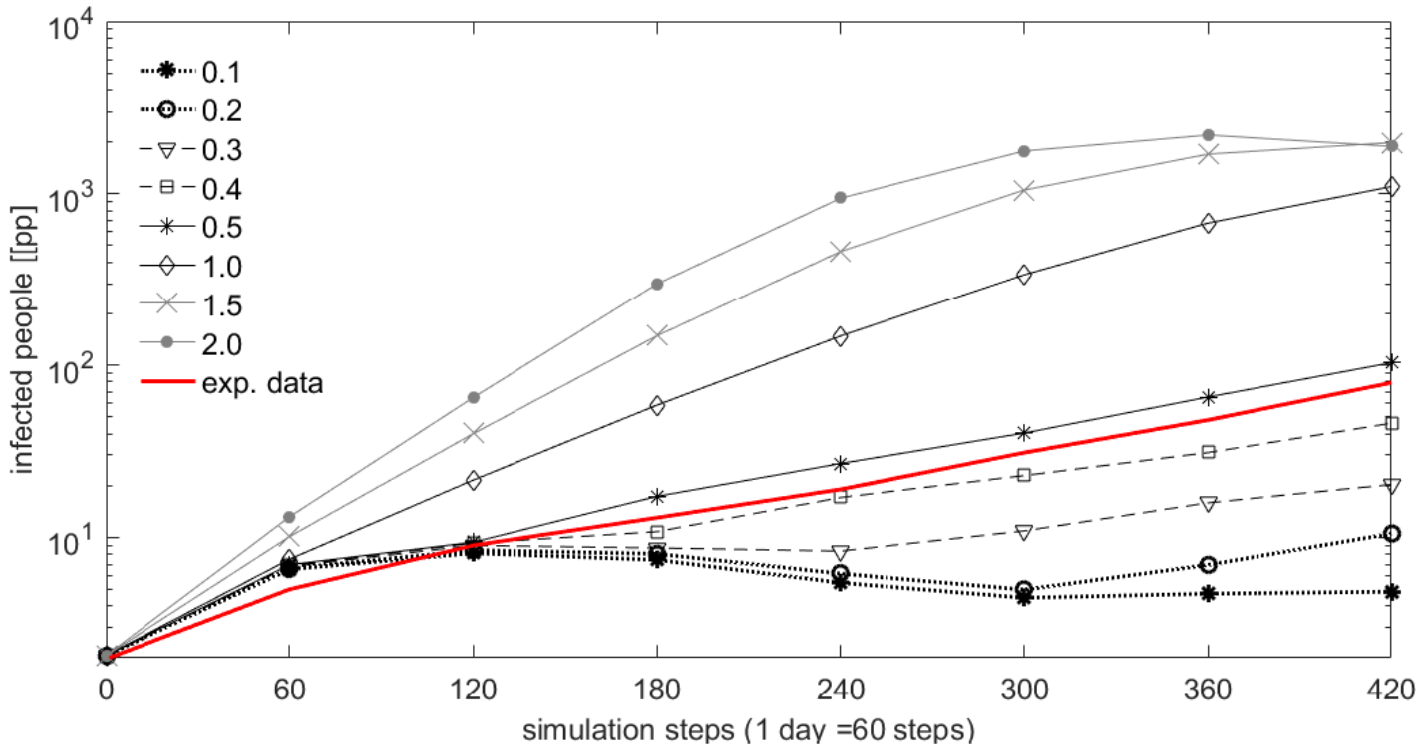

Figure 2

Comparison between the experimental data from the Diamond Princess cruise (red line) and the simulation results, for the main formcoeff values according to their trend. Infected people are represented by logarithm scale.

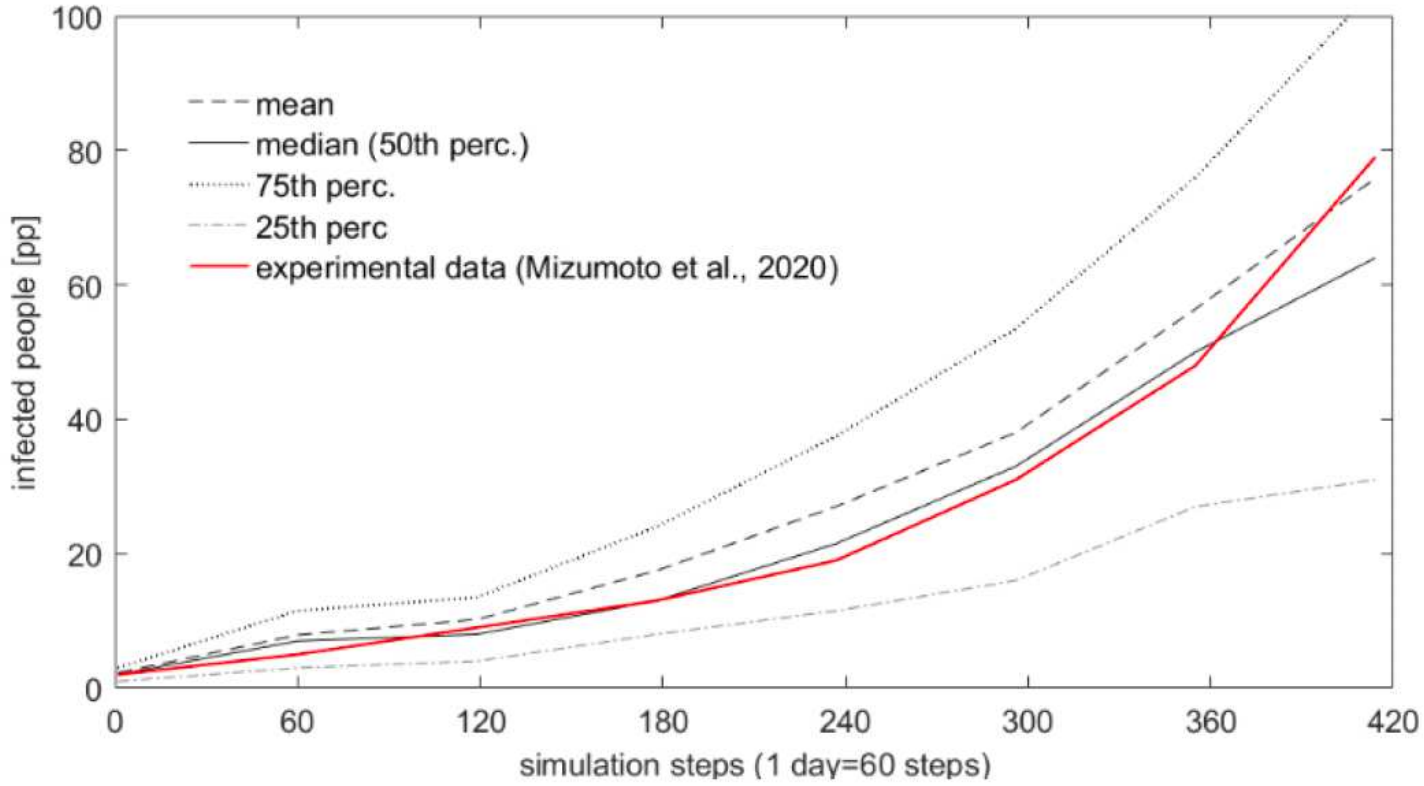

Figure 3

Comparison between the experimental data from the Diamond Princess cruise (red line) and the simulation results, for the best formcoeff values (0.5), by considering different percentiles and mean data.

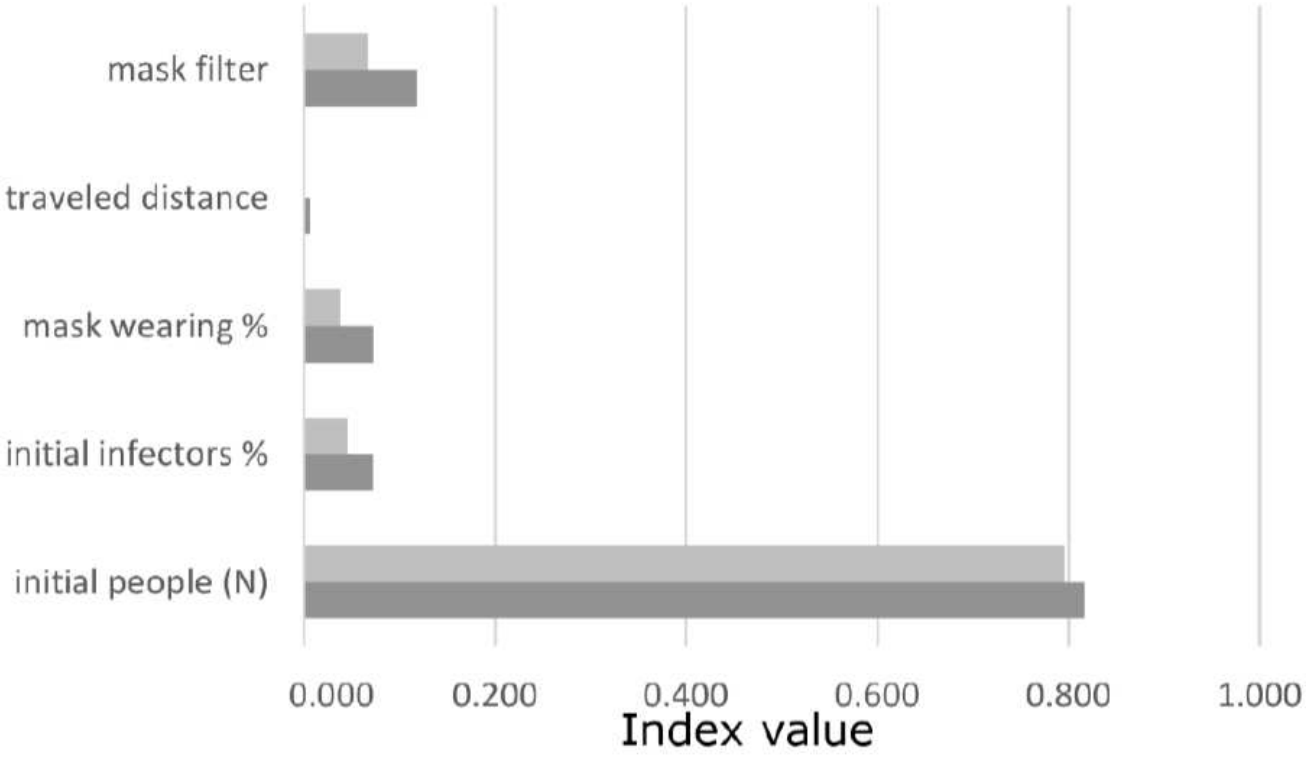

	initial people (N)	initial infectors %	mask wearing %	traveled distance	mask filter
Sobol First Order Index	0.796	0.045	0.038	-	0.066
Sobol Total Order Index	0.817	0.072	0.073	0.006	0.118

Figure 4

Total order sensitivity indices (STi – dark grey) and the first-order sensitivity indices (SFi– light grey) for the considered parameters.

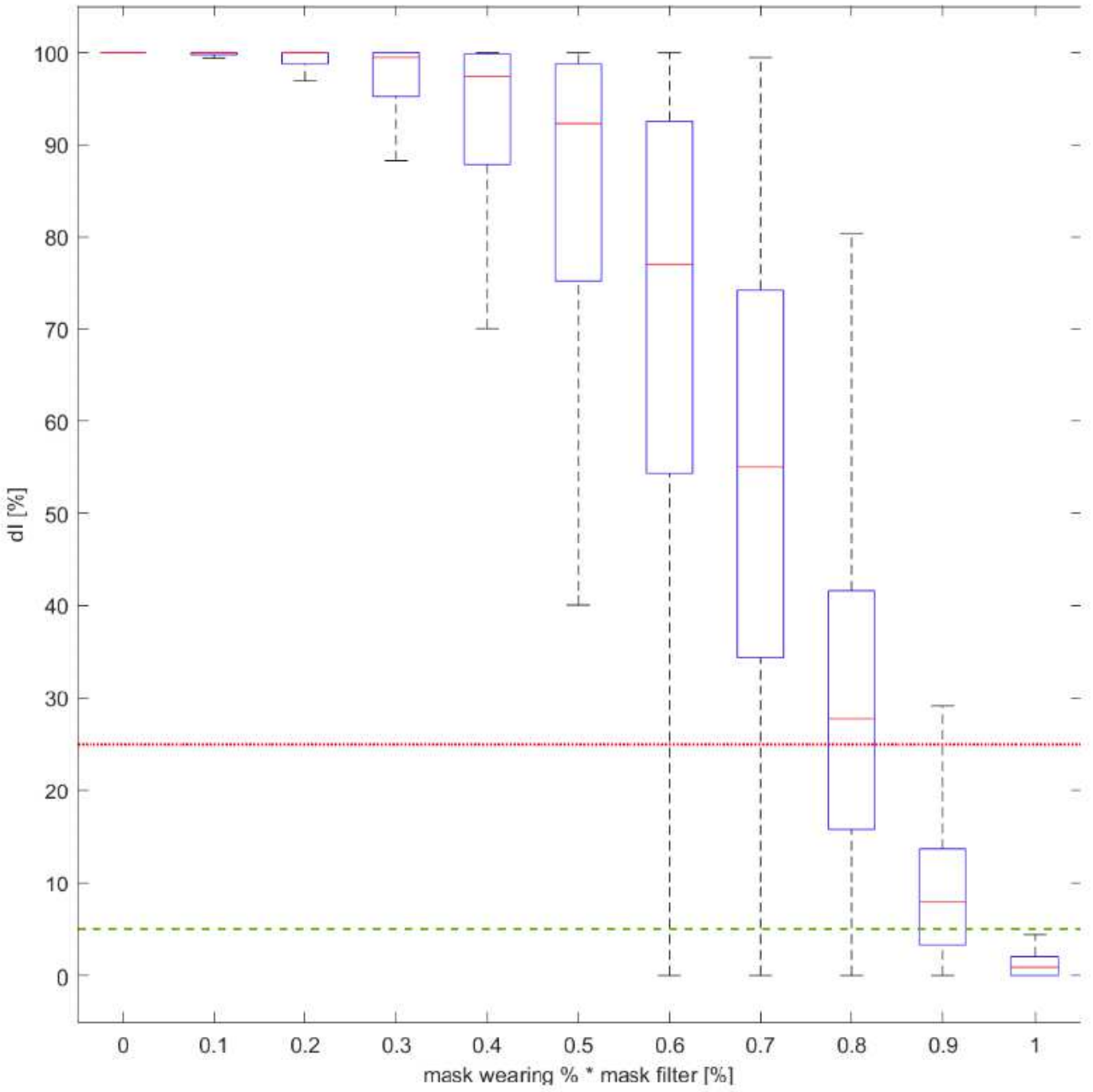

Figure 5

Boxplot dI values distribution at the last simulation step for the whole sample, with respect to the effects related to mask (mask filter and mask wearing %). dI acceptable thresholds are defined at dI=5% (dashed green line) and 25% (continuous red line).

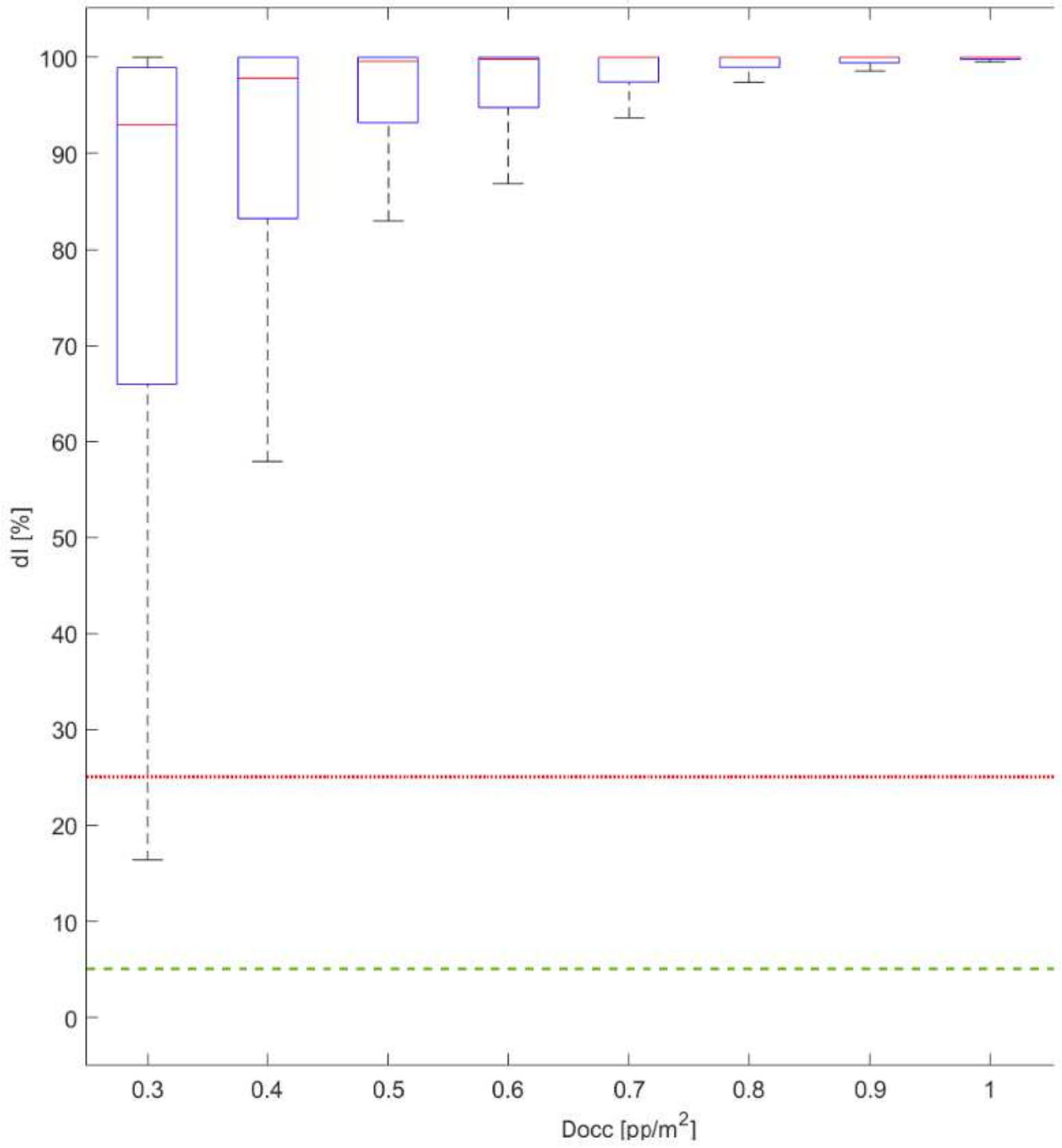

Figure 6

Boxplot dI values distribution at the last simulation step for the whole sample, with respect to the effect of occupants' density Docc values discretized by 0.1pp/m2. dI acceptable thresholds are defined at dI=5% (dashed green line) and 25% (continuous red line).

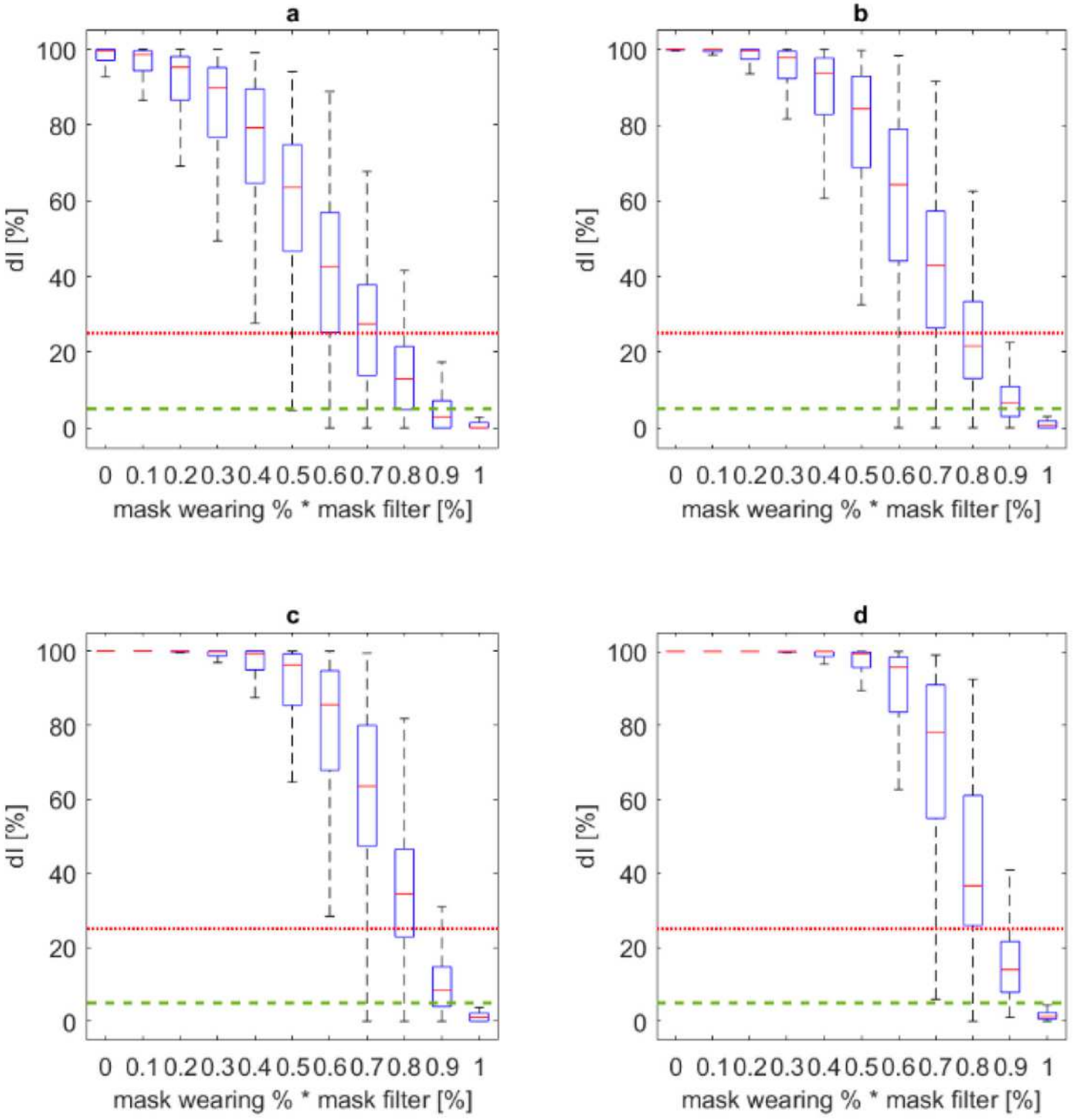

Figure 7

Boxplot dI values distribution at the last simulation step for the whole sample, with respect to the effects of different density classes: a) Docc≤0.3pp/m2; b) 0.3pp/m2<Docc≤0.5pp/m2; c) 0.5pp/m2<Docc≤0.7pp/m2; d) 0.7pp/m2<Docc≤1.0pp/m2 . Values are traced according to the overall mask effect. dI acceptable thresholds are defined at dI=5% (dashed green line) and 25% (continuous red line).

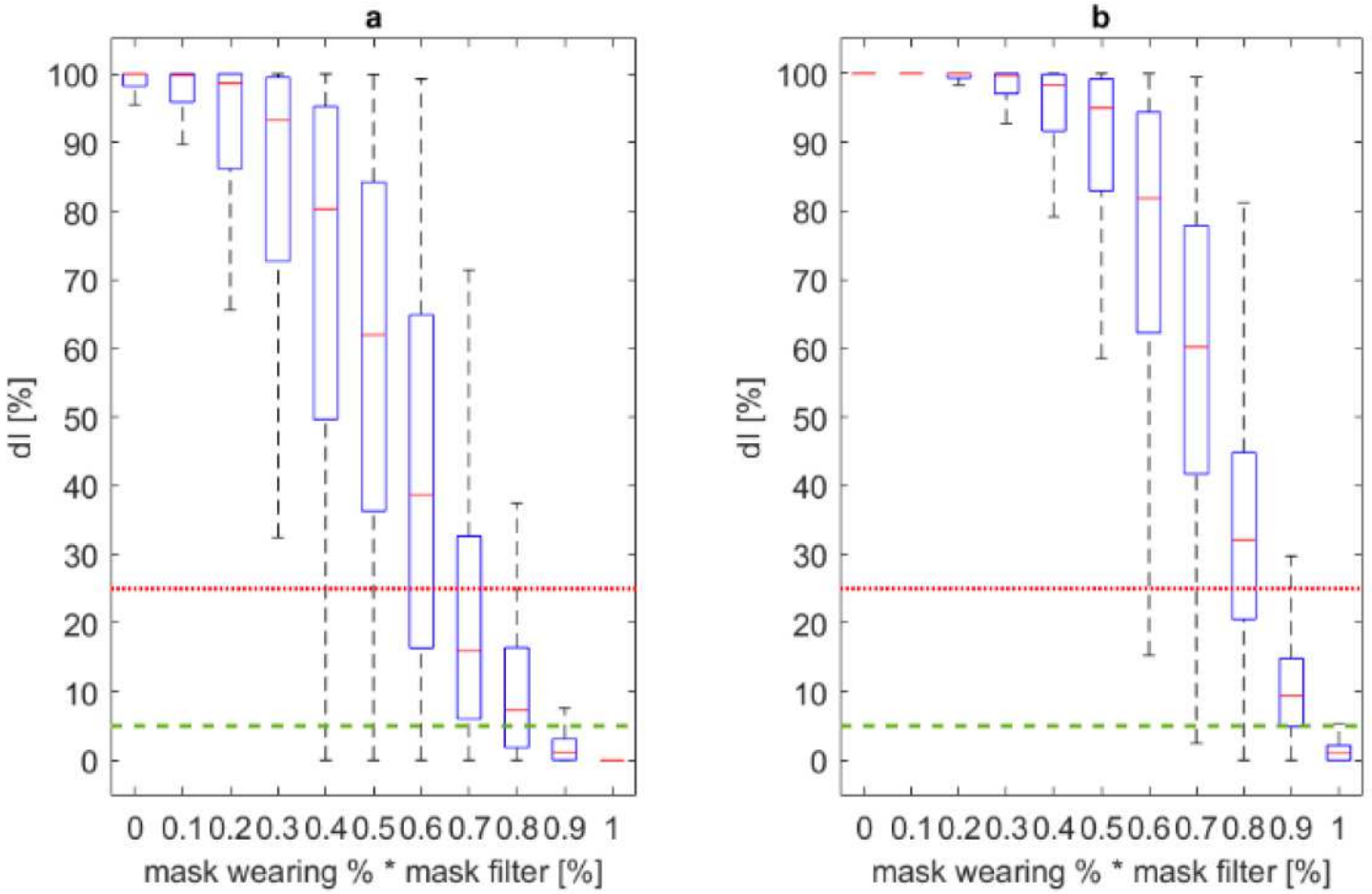

Figure 8

Boxplot dI values distribution at the last simulation step for the whole sample, with respect to: a) access control strategies implemented and b) no access control strategies implemented. Values are traced according to the overall mask effect. dI acceptable thresholds are defined at dI=5% (dashed green line) and 25% (continuous red line).

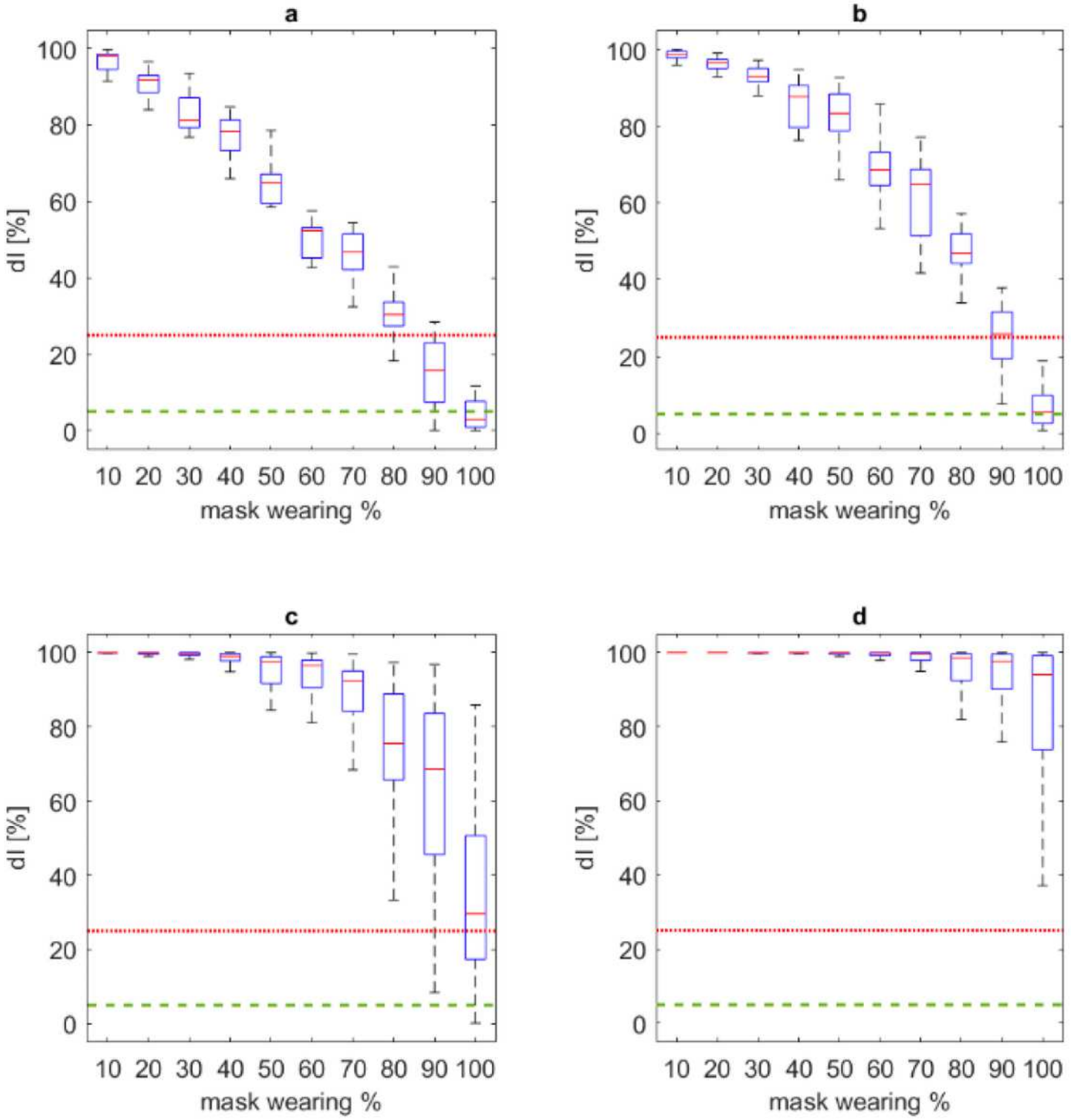

Figure 9

Boxplot dI values distribution at the last simulation step for maximum building capacity, in respect to the effects of different mask filter classes: a) FFP3; b) FFP2; c) FFP1; d) surgical mask. The Boxplot representation is offered by distinguishing the different mask wearing % classes. dI acceptable thresholds are defined at dI=5% (dashed green line) and 25% (continuous red line).

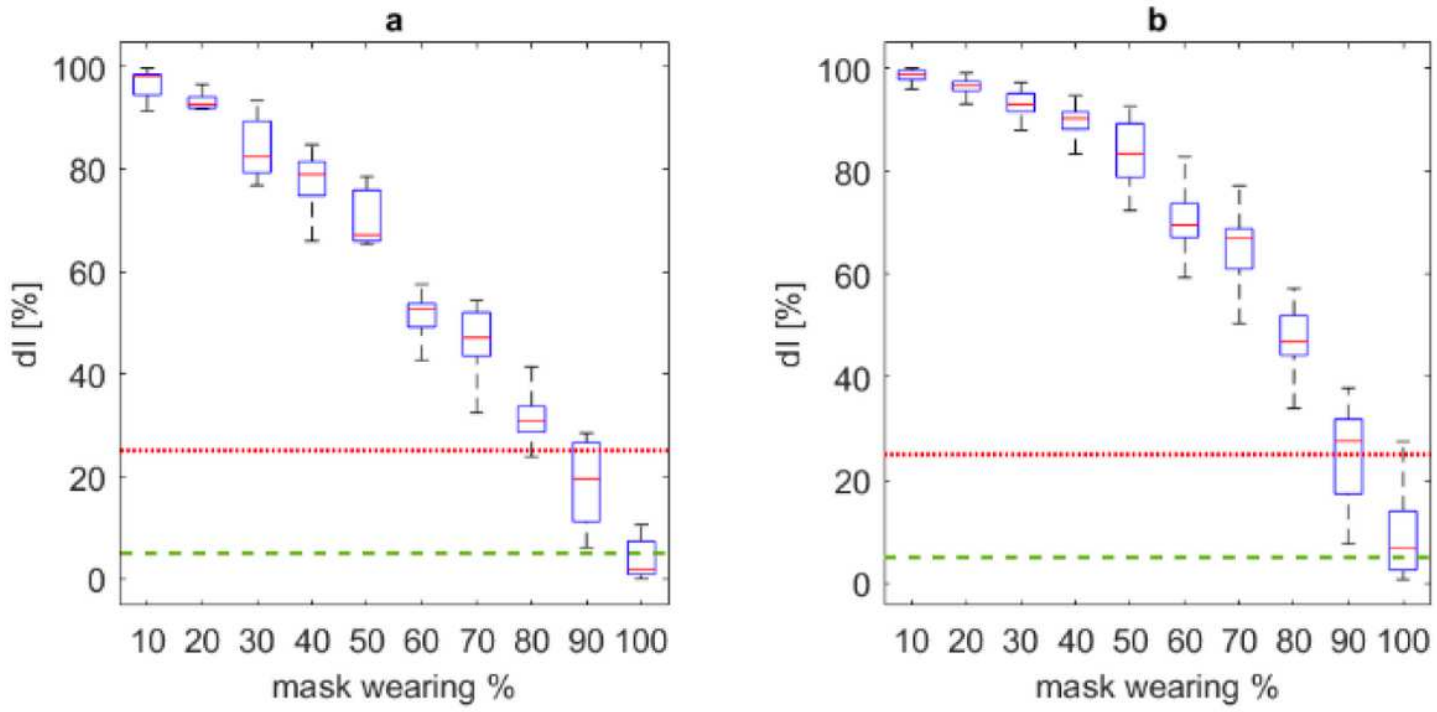

Figure 10

Boxplot dI values distribution at the last simulation step for maximum building capacity in no access control strategies conditions, in respect to the effects of different mask filter classes: a) FFP3; b) FFP2. The Boxplot representation is offered by distinguishing the different mask wearing % classes. dI acceptable thresholds are defined at dI=5% (dashed green line) and 25% (continuous red line).

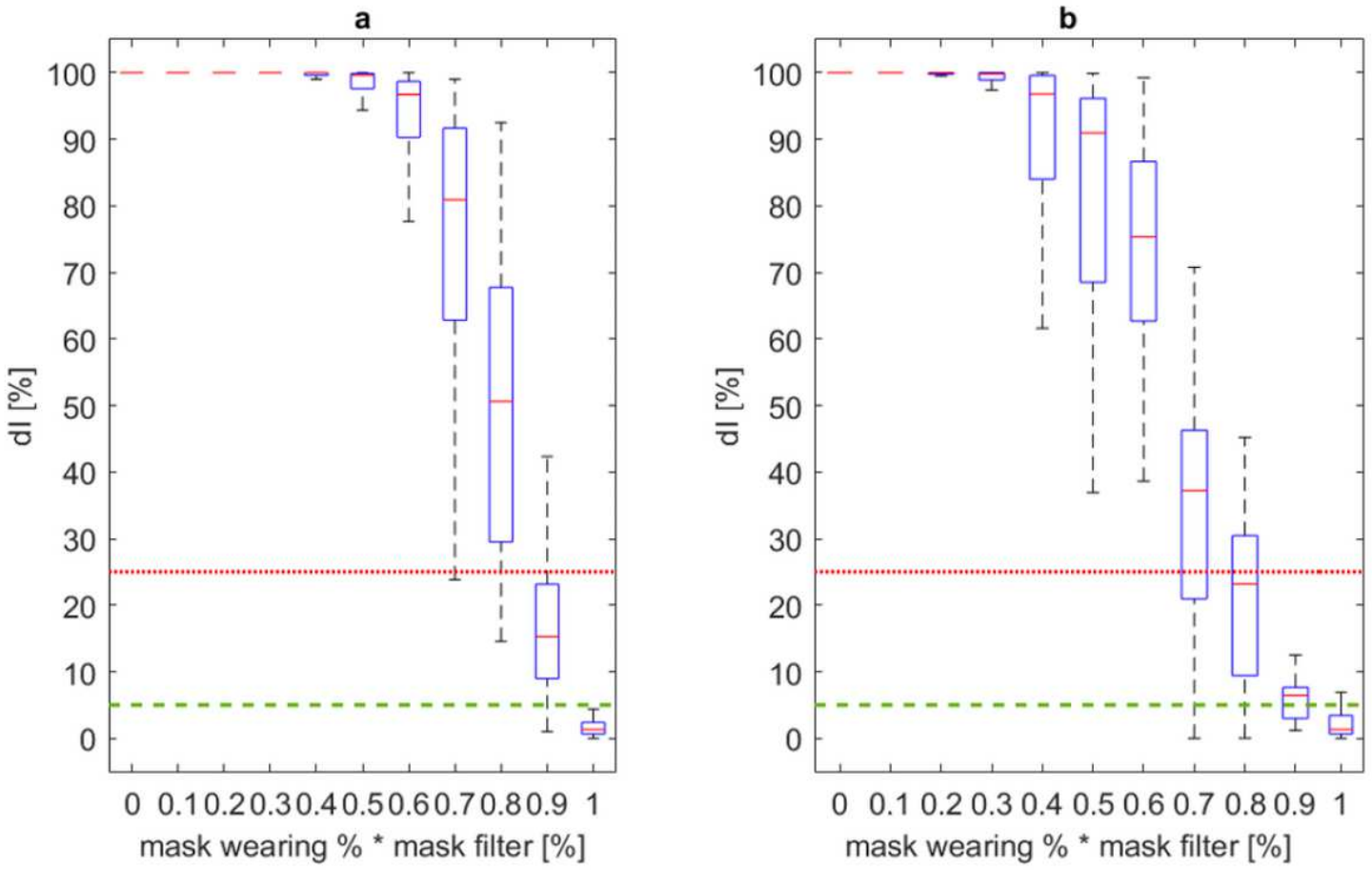

Figure 11

Boxplot dI values distribution at the last simulation step for maximum building capacity, in respect to: a) access control strategies implemented and b) no access control strategies implemented. Values are traced according to the overall mask effect. dI acceptable thresholds are defined at dI=5% (dashed green line) and 25% (continuous red line).

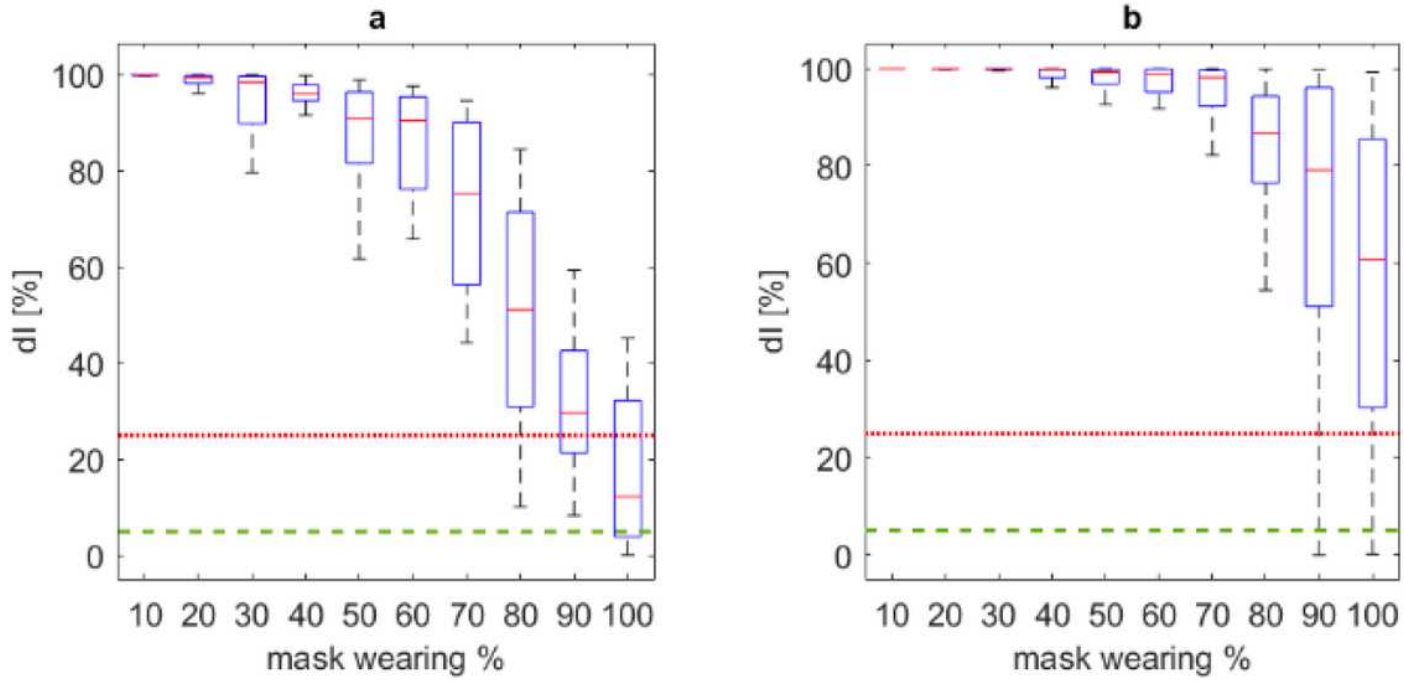

Figure 12

Boxplot dI values distribution at the last simulation step for maximum building capacity when access control strategies are considered, in respect to the effects of different mask filter classes: a) FFP1; b) surgical masks. The Boxplot representation is offered by distinguishing the different mask wearing % classes. dI acceptable thresholds are defined at dI=5% (dashed green line) and 25% (continuous red line).

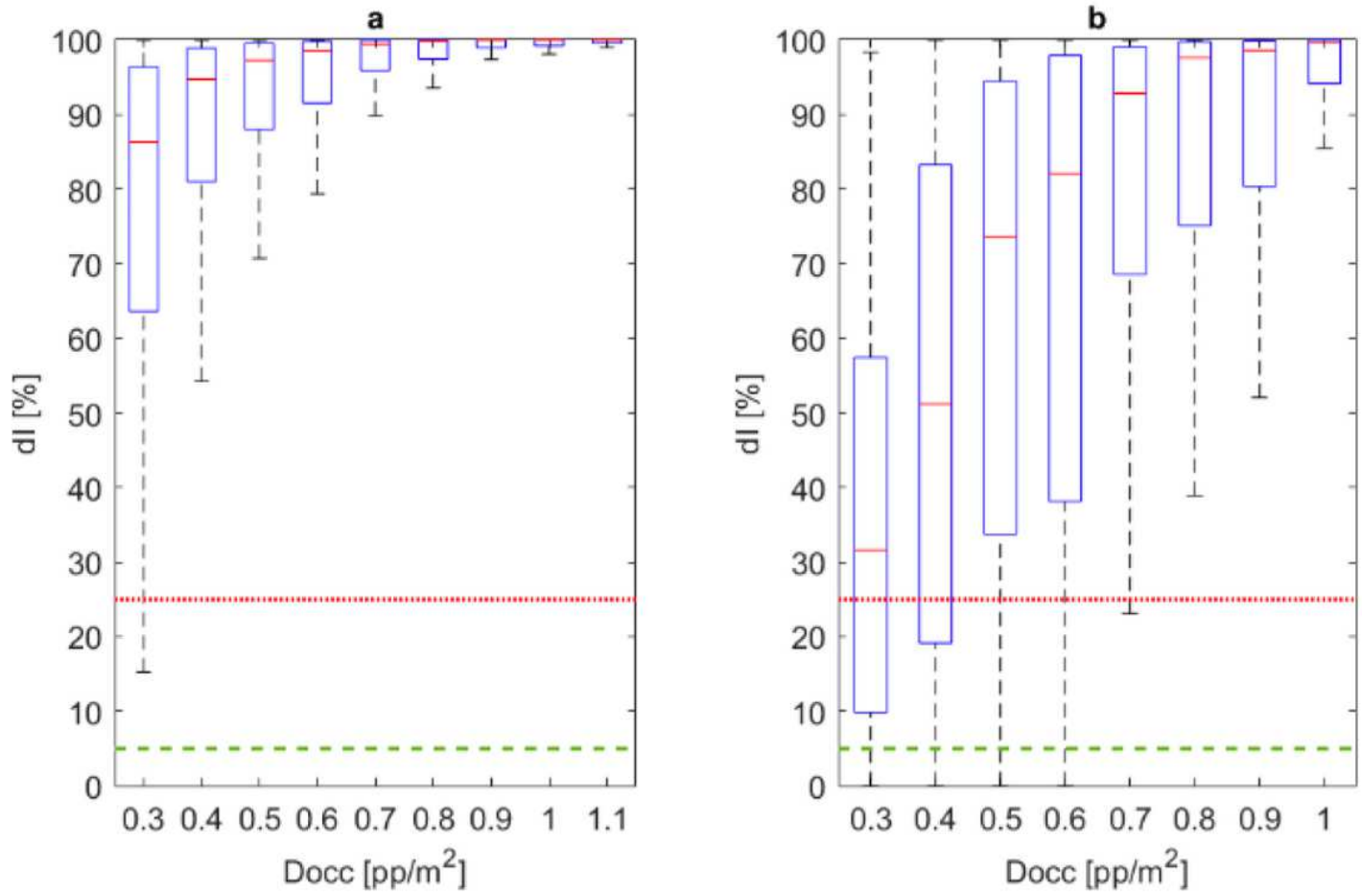

Figure 13

Boxplot dI values distribution at the last simulation step for surgical masks implementation in relation to the occupants' density Docc classes, with respect to: a) no access control strategies implemented; b) access control strategies implemented. Data are offered regardless of the mask wearing % classes. dI acceptable thresholds are defined at dI=5% (dashed green line) and 25% (continuous red line).

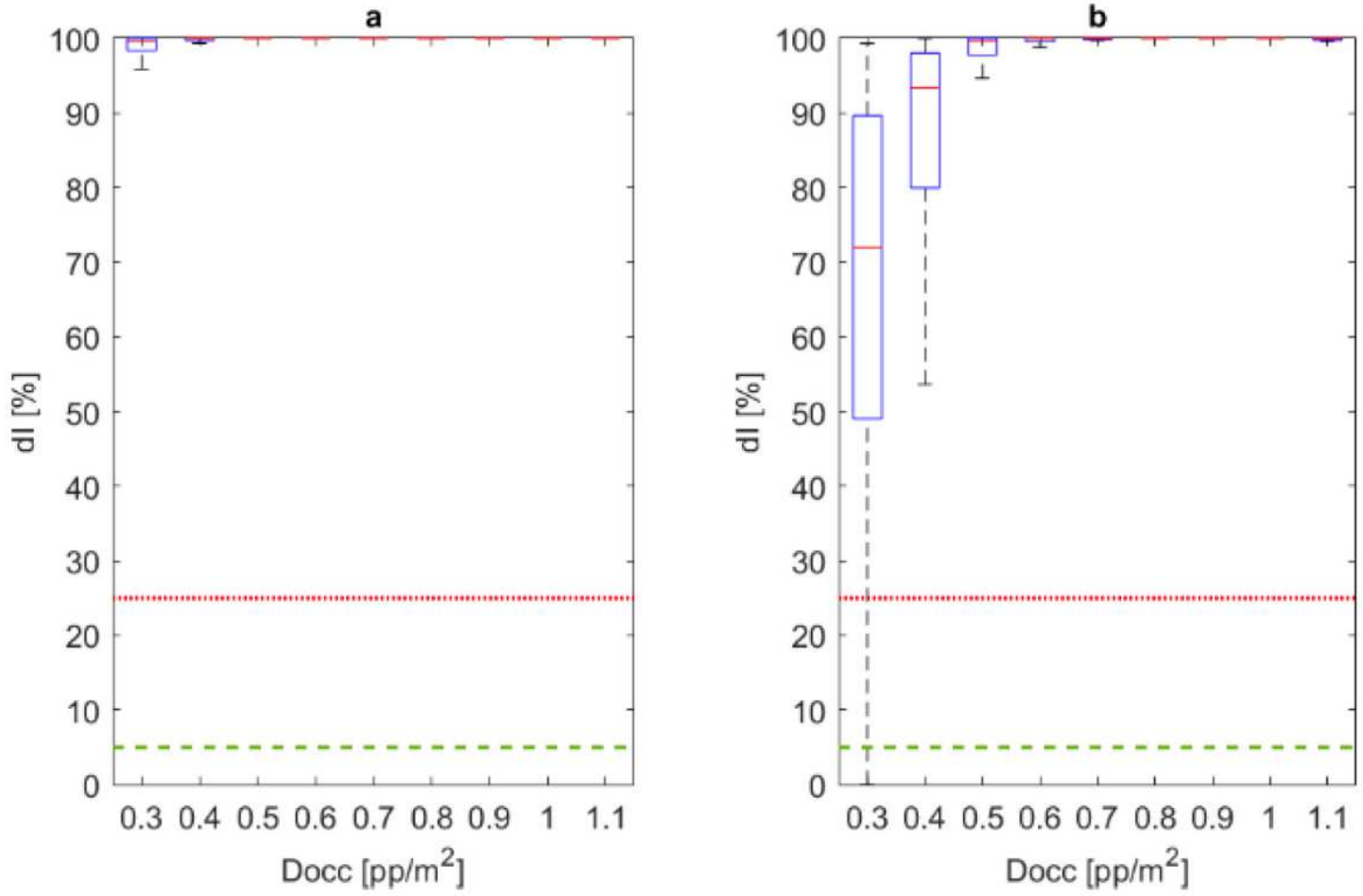

Figure 14

Boxplot dI values distribution at the last simulation step for non-standards protection (0 to 0.25, compare to Table 1) solutions, in relation to the occupants' density Docc classes, with respect to: a) no access control strategies implemented; b) access control strategies implemented. Data are offered regardless of the mask wearing % classes. dI acceptable thresholds are defined at dI=5% (dashed green line) and 25% (continuous red line).

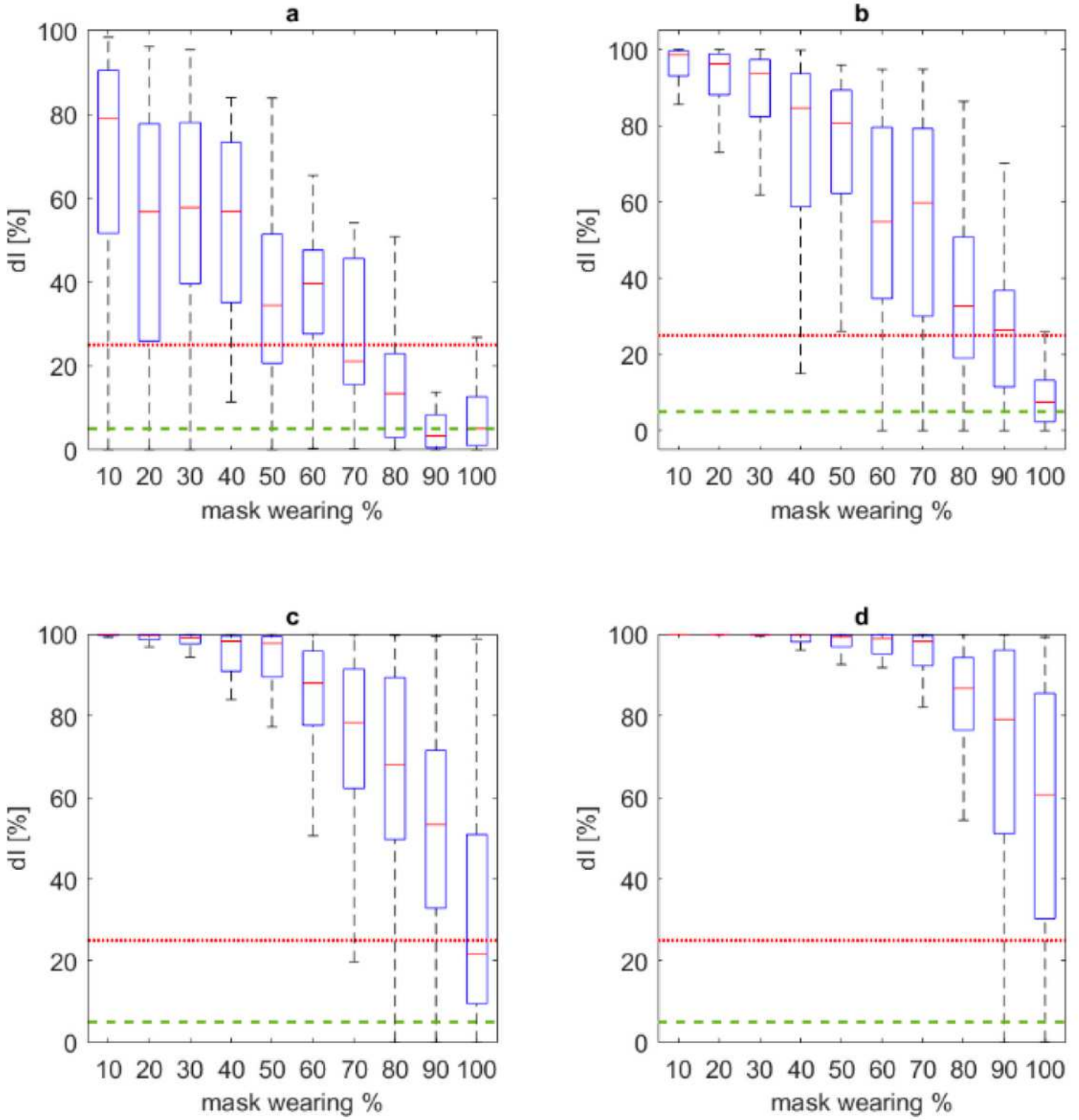

Figure 15

Boxplot dI values distribution at the last simulation step for surgical mask implementation scenarios, with respect to the effects of different density classes: a) Docc≤0.3pp/m2; b) 0.3pp/m2<Docc≤0.5pp/m2; c) 0.5pp/m2<Docc≤0.7pp/m2; d) 0.7pp/m2<Docc≤1.0pp/m2 . Values are traced according to the overall mask effect. dI acceptable thresholds are defined at dI=5% (dashed green line) and 25% (continuous red line).

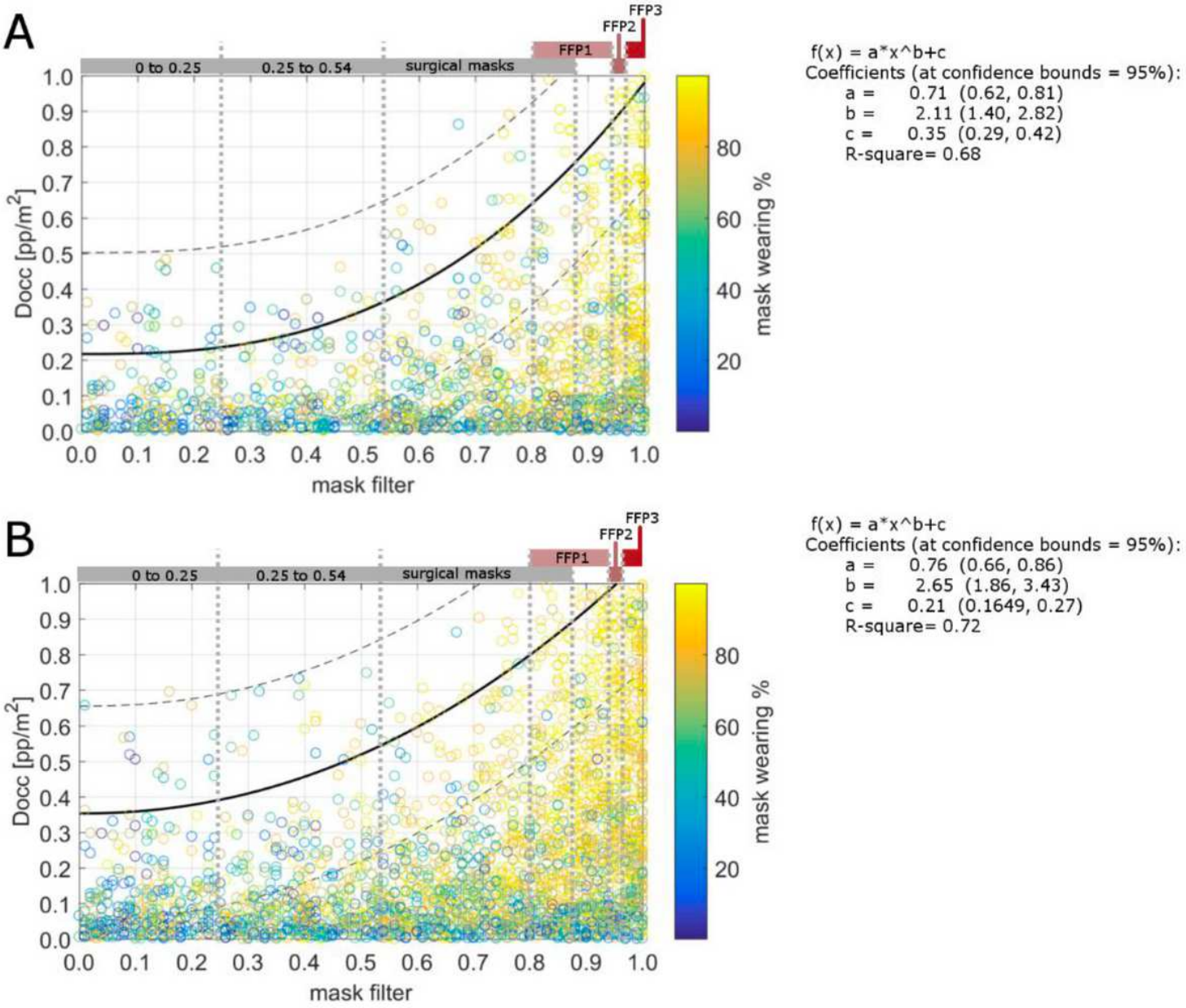

Figure 16

Mask filter-Docc correlation for all the pairs related to a) dI≤5% and b) dI≤25%. The pairs' colour is related to the mask wearing %. Regression curves (axb+c) are shown by providing 95% of confidence intervals regression (dashed lines; see equation coefficients on the right of each panel). Mask filter classes are also shown in the upper part of the graphs.